Proc. R. Soc. Lond. A **412**, 93–123 (1987)
Printed in Great Britain

Gaussian wave packets in inhomogeneous media with curved interfaces

By A. N. Norris[1], B. S. White[2] and J. R. Schrieffer[3]

[1] *Rutgers University, Department of Mechanics and Materials Science, P.O. Box* 909, *Piscataway, New Jersey* 08855, *U.S.A.*

[2] *Exxon Research and Engineering Co., Route* 22 *East, Annandale, New Jersey* 08801, *U.S.A.*

[3] *Institute for Theoretical Physics, University of California, Santa Barbara, California* 93106, *U.S.A.*

(*Communicated by Sir James Lighthill, F.R.S. – Received* 14 *August* 1986)

Time-dependent particle-like pulses are considered as asymptotic solutions of the classical wave equation. The wave packets are localized in space with gaussian envelopes. The pulse centres propagate along the rays of the wave equation, and the envelope parameters satisfy evolution equations very similar to the ray equations for time-harmonic disturbances. However, the present theory contains an extra degree of freedom not found in the time-harmonic theory. Explicit results are presented for media with constant velocity gradients, and interesting new phenomena are identified. For example, a pulse that is initially long in the direction of propagation and comparatively narrow in the orthogonal direction, maintains its initial spatial orientation even as the propagation direction rotates. The reflection and transmission of a pulse incident upon an interface are also discussed. The various theoretical results are illustrated by numerical simulations. This method of solution could be very useful for fast forward modelling in large-scale structures. It is formulated explicitly in the time domain and does not suffer from unphysical singularities at caustics.

1. Introduction

Time-dependent gaussian wave packets have been found to give a good description of certain problems relating to the classical wave equation and to the Schrödinger equation. This paper concentrates on the application of wave packets to the wave equation for an inhomogeneous acoustic medium. Extensions of the method to vector wave equations for elasticity and electromagnetism are straightforward.

Hagedorn (1984) showed that a gaussian wave packet is an asymptotic solution of the time-dependent wave equation. The packet is localized in space with a gaussian envelope. The centre of the gaussian wave packet, hereafter referred to as a GWP, propagates along the rays or characteristics of the wave equation. The parameters describing the packet evolve with time according to equations deduced by Hagedorn.

Previous asymptotic solutions in the form of beams (Cerveny 1983; Popov 1982) have usually been formulated in the frequency domain, rather than explicitly in the time domain. One exception is Berlanger (1984), but his solution has infinite energy and is more like a plane-wave solution than a localized packet. Some applications of the gaussian beam method due to Popov (1982), Cerveny (1983) and others have been given in the time domain. For example, Cerveny (1983) discussed the propagation of a Gabor wavelet with a gaussian envelope. The difference between this type of solution and the GWP rests with the initial conditions. The initial data for the gaussian pulses of Cerveny (1983) are given on a surface in space for all time. On the other hand, the GWP as discussed here and by Hagedorn (1984) is prescribed at a given initial time over all space. In practice, because the GWP is localized in space, one only needs to know the initial pulse in a neighbourhood of the wave packet centre. Obviously, there is a lot of overlap between the present theory and that of gaussian beams. A full discussion and comparison of the two theories is left until later. The purpose of the present paper is to emphasize the basic theory of wave packets and their use in practical applications.

The present theory is valid asymptotically in the limit that the central frequency of the packet is very large. The equations of evolution are derived in §2 after assuming a time-dependent Ansatz. The derivation is more general than Hagedorn's (1984), who initially assumes a GWP form for the solution. It is shown here that the GWP arises naturally as the only possible localized solution to the evolution equations. The analysis uses Hamilton–Jacobi theory extended to allow for complex spatial positions. Of course, all physically significant results are evaluated in real space, but the idea of analytically extended space is found to be useful. For example, the gaussian beam theory of Cerveny (1983) is usually derived from the parabolic equation. White *et al.* (1987) showed that the introduction of the parabolic equation is unnecessary and that time-harmonic gaussian beam solutions follow naturally from ray theory extended into complex space. Similarly, Norris (1986) proved that the use of point sources in complex space provides an exact basis for the asymptotic beam superposition integral of Cerveny (1983). One can also obtain useful results by extending time to complex values, but this will not be necessary in the present paper.

The evolution equations for the GWP are a system of ordinary differential equations in time. Some general properties of the solution are presented in §3. In §4, the equations are formulated in terms of a specific coordinate system that moves with the ray. It is known (Hubral 1980) that tractable solutions to the ray equations can be obtained in media with constant velocity gradients. The same applies to GWPs in such media, and explicit results are given in §5. The analytical results suggest new and interesting phenomena associated with wave packets in heterogeneous media. In general, the 'particle path' associated with the packet centre follows the useful ray path of geometrical optics. However, the packet envelope can rotate relative to the propagation direction. Thus, a pulse that is initially long in the direction of propagation and narrow in the orthogonal direction tends to maintain the initial orientation of the packet envelope, even though the propagation direction rotates. This effect is demonstrated by numerical example. Finally, the reflection and transmission of a GWP from an interface between two different media are discussed in §6. The procedure is illustrated by application to a two-dimensional problem of scattering from a circular region of higher velocity.

There is much similarity between the present asymptotic solution of the wave equation and time-dependent solutions to the Schrödinger equation. Thus, Synge (1972) proposed an exact GWP type of solution to the Schrödinger equation for a free particle. He modified the fundamental solution by changing the origins of space and time to complex values, thereby removing the mathematical singularities from real space and time. Recently, time-dependent gaussian wave packets have been used extensively for certain problems in quantum chemistry, such as photoexcitation and photodissociation of small molecules, as well as Raman scattering processes. Much of the development in these areas is due to E. Heller (1975), who took the original idea of a gaussian solution and subsequently developed it for many different applications. Various schemes have been proposed that involve minimizing functionals of the wave function. It is shown in Appendix A how these methods relate to the present method, which can be formulated as the minimization of an action integral.

2. Time-dependent wave packets

2.1. *Equations of motion*

The three-dimensional scalar wave equation for an inhomogeneous medium is

$$\nabla\mu\cdot\nabla u-\rho u_{tt}=0, \tag{2.1}$$

where the subscript t denotes differentiation with respect to time. For example, in two dimensions (2.1) is the equation for simple harmonic (SH) motion, where u is the out-of-plane motion, μ the shear modulus and ρ the density. Equation (2.1) also models acoustic waves in three dimensions, where u represents the pressure, $1/\mu$ the density, and ρ the bulk compressibility. In either case, μ and ρ may be functions of position $\boldsymbol{x}$.

We seek solutions in the form of travelling wave packets. At any instant in time the packet should be localized in space. Of course, as the packet propagates, we expect it to scatter from interfaces and regions of discontinuity, with the result that after a while there may exist several localized packets (see §6).

Consider the Ansatz

$$u = V(\boldsymbol{x},t)\,\mathrm{e}^{\mathrm{i}\omega\phi(\boldsymbol{x},\,t)}, \tag{2.2}$$

where $\omega \gg 1$ is an arbitrary parameter. We allow both V and ϕ to be complex. The form of the present Ansatz is motivated by results for high-frequency solutions to the inhomogeneous Helmholtz equation corresponding to (2.1). Thus, although ω is a free parameter in the present theory, it can be understood as the centre frequency of the wave packet. Note that in ordinary ray theory, the phase is of the form $\phi(\boldsymbol{x},t) = \Phi(\boldsymbol{x})-t$, where Φ is real. The gaussian beam-summation method (Popov 1982; Cerveny 1983; White *et al.* 1985) uses individual beams or rays for which the phase is of the same form as in ordinary ray theory, but Φ is allowed to be complex. In the present paper, the position is considered as a complex vector. Real space is analytically continued and one can generalize ordinary ray theory into complex space (Keller & Streifer 1971; Felsen 1976). Rays still propagate in straight lines in homogeneous media, but can now propagate through complex space, possibly intersecting real space at isolated points. A ray starting at a real point, with a real initial direction, remains in real space. Similarly, a ray starting at a complex point with a real direction initially, also remains in complex space. However, the Fermet or stationary ray between two real points may not always be a real ray. For example, a point on the dark side of a caustic can only be reached by a complex ray. Every real ray has an associated neighbouring fan of complex rays. These rays can be approximated by using a paraxial approximation about the central real ray. Thus, explicit ray tracing can be confined to real rays; complex rays are then considered implicitly through the paraxial approximation. This procedure is of course an approximation to full complex ray tracing. The latter can be defined formally, but is computationally difficult, requiring two-point ray tracing algorithms through complex space.

Inserting u of (2.2) into (2.1) and equating terms of equal power in $(\mathrm{i}\omega)$, yields to highest order the 'eiconal' equation

$$\phi_t^2 = c^2\,|\nabla\phi|^2, \tag{2.3}$$

where the wave speed is

$$c(\boldsymbol{x}) = (\mu/\rho)^{\frac{1}{2}}. \tag{2.4}$$

For any complex vector $\boldsymbol{v}$ define the complex number $|\boldsymbol{v}| = (\boldsymbol{v}\cdot\boldsymbol{v})^{\frac{1}{2}}$, where the branch cut is defined by $\operatorname{Re}(\ )^{\frac{1}{2}} \geqslant 0$. If a is a complex number, define the positive real number $|a|$ as the magnitude of a. The next term in the wave equation expansion gives the transport equation,

$$c^2\nabla^2\phi + 2c^2\frac{\nabla V}{V}\cdot\nabla\phi + c^2\frac{\nabla\mu}{\mu}\cdot\nabla\phi - \phi_{tt} - \frac{2}{V}\,V_t\,\phi_t = 0. \tag{2.5}$$

In general, (2.3)–(2.5) are defined for $\boldsymbol{x}$ and t complex; however, for the rest of the paper t is assumed as real.

2.2. *The eiconal equation and ray parameters*

We now introduce ray parameters. In general, the rays are defined in complex space. Real rays, i.e. rays in real space, will be specifically considered later. Let t be the ray parameter along a particular ray. The arc length parameter s is usually used instead of time to define position along a ray. However, time is chosen here to emphasize the time dependent aspect of our solution. Let $s = s_0$ at $t = t_0$, then at subsequent times, the relation between t and s is

$$s = s_0 + \int_{t_0}^{t} c(\boldsymbol{y}(t))\,\mathrm{d}t. \tag{2.6}$$

Here, $\boldsymbol{y}(t)$ is the ray position at time t. It follows by choosing one of the two characteristics of (2.3). The root

$$\phi_t + c|\boldsymbol{p}| = 0 \tag{2.7}$$

is chosen, where the (complex) vector $\boldsymbol{p}$ is defined

$$\boldsymbol{p} = \nabla\phi. \tag{2.8}$$

Now consider the hamiltonian $H = \phi_t + c|\boldsymbol{p}|$ with $\boldsymbol{y}$ and $\boldsymbol{p}$ as conjugate variable, for which Hamilton's equations are:

$$\dot{\boldsymbol{y}}(t) = c(\boldsymbol{y}(t))\,\bar{\boldsymbol{p}}(t), \tag{2.9a}$$

$$\dot{\bar{\boldsymbol{p}}}(t) = -\boldsymbol{P}_{\perp}(t)\,\nabla c, \tag{2.9b}$$

with initial conditions at $t = t_0$,

$$\boldsymbol{y}(t_0) = \boldsymbol{y}_0, \tag{2.9c}$$

$$\boldsymbol{p}(t_0) = \boldsymbol{p}_0. \tag{2.9d}$$

The dot over a quantity denotes the total derivative with respect to time $\mathrm{d}/\mathrm{d}t$, as distinct from the partial derivative $\partial/\partial t$. The initial ray position $\boldsymbol{y}_0$ and direction $\boldsymbol{p}_0$ can be complex. Real rays are obtained only if both are real. Also,

$$\bar{\boldsymbol{p}} = \boldsymbol{p}/|\boldsymbol{p}| \tag{2.10}$$

is the unit vector in the ray direction, and

$$P_{\perp}(t) = \boldsymbol{I} - \bar{\boldsymbol{p}}\bar{\boldsymbol{p}}^T \tag{2.11}$$

projects vectors on to the surface orthogonal to the ray direction. This surface corresponds to the 'wavefront' in normal time-harmonic ray theory. It is usually defined as a surface of constant phase. It has no particular significance in the present theory, because there is no surface of constant phase, only a single point. This follows from the fact that the total derivative of ϕ along a ray follows from (2.9a) as

$$\begin{aligned}\dot{\phi} &= \phi_t + \dot{\boldsymbol{y}}\cdot\nabla\phi \\ &= 0.\end{aligned} \tag{2.12}$$

Hence, the phase ϕ is constant along a ray.

Note also that $|\boldsymbol{p}|$, which is in general a complex number, is not necessarily equal to $1/c$, as is the case in the time-harmonic problem. However, it follows from (2.12) that $\mathrm{d}(c|\boldsymbol{p}|)/\mathrm{d}t = 0$, and so

$$|\boldsymbol{p}(t)| = |\boldsymbol{p}(t_0)|\frac{c(\boldsymbol{y}(t_0))}{c(\boldsymbol{y}(t))}. \tag{2.13}$$

This freedom in defining $|\boldsymbol{p}|$ is due to the arbitrary definition of ω, the frequency. Without any loss of generality we now specify the normalization $|\boldsymbol{p}| = 1/c$ for subsequent use.

2.3. *The transport equation*

Consider the transport equation (2.5). From (2.9a), it follows that

$$\nabla\mu\cdot\nabla\phi = \frac{1}{c^2}\frac{\mathrm{d}\mu}{\mathrm{d}t}. \tag{2.14}$$

The quantity ϕ_{tt} in (2.5) follows by differentiating (2.7) with respect to t and by using the result $\mathrm{d}(c|\boldsymbol{p}|)/\mathrm{d}t = 0$ to obtain

$$\phi_{tt} = c^2\bar{\boldsymbol{p}}\cdot\nabla\nabla\phi\cdot\bar{\boldsymbol{p}} + \bar{\boldsymbol{p}}\cdot\nabla c. \tag{2.15}$$

Note that, in ordinary ray theory, the phase is of the form $\phi(\boldsymbol{x}, t) = \Phi(\boldsymbol{x}) - t$, and therefore $\phi_{tt} = 0$. Defining the symmetric complex matrix $\boldsymbol{M}(t)$ as

$$\boldsymbol{M} = \nabla\nabla\phi(\boldsymbol{y}(t), t) \tag{2.16}$$

the transport equation becomes

$$\frac{\mathrm{d}}{\mathrm{d}t}\lg\left(\frac{\mu V^2}{c}\right) + \mathrm{tr}\,(c^2\boldsymbol{P}_\perp\boldsymbol{M}) = 0. \tag{2.17}$$

Next, introduce the 3×3 complex matrix $\boldsymbol{A}(t)$, which satisfies

$$\dot{\boldsymbol{A}} = \bar{\boldsymbol{p}}\nabla c^T\boldsymbol{A} + c^2\boldsymbol{P}_\perp\boldsymbol{M}\boldsymbol{A} \tag{2.18}$$

with initial conditions $\boldsymbol{A}(t_0) = \boldsymbol{A}_0$. The genesis of (2.18) will be explained shortly. The matrix $\boldsymbol{A}$ is the analog of the 2×2 wavefront-area matrix in the time-harmonic problem. However, unlike normal ray theory, $\boldsymbol{A}$ may be complex. In this sense, $\boldsymbol{A}$ is more akin to the complex 2×2 matrix exployed in the gaussian beam method (Cerveny 1983); however, $\boldsymbol{A}$ is now a 3×3 matrix. It follows from (2.18) that

$$\frac{\mathrm{d}}{\mathrm{d}t}\lg\left[\det(\boldsymbol{A})\right] - \frac{\mathrm{d}}{\mathrm{d}t}\lg(c) = \mathrm{tr}\,(c^2\boldsymbol{P}_\perp\boldsymbol{M}). \tag{2.19}$$

Equations (2.17) and (2.19), combined, give

$$V(\boldsymbol{y}(t), t) = V(t_0)\left[\frac{\rho(\boldsymbol{y}(t_0))\,\det(\boldsymbol{A}(t_0))}{\rho(\boldsymbol{y}(t))\,\det(\boldsymbol{A}(t))}\right]^{\frac{1}{2}}. \tag{2.20}$$

Comparison of (2.19) with (25) of Karal & Keller (1959) shows that $\boldsymbol{A}/c$ is actually the analog of the wavefront-area matrix. The origin of the latter comes from the idea of a ray-tube area associated with a bundle of rays.

It remains to get an equation for the evolution of $\boldsymbol{M}(t)$. Consider the variational equations corresponding to the ray equations (2.9a) and (2.9b). Let $\boldsymbol{a}$ be some vector parameter, e.g. the initial ray position $\boldsymbol{y}(t_0)$. Define the 3×3 complex matrices $\boldsymbol{A}(t)$ and $\boldsymbol{B}(t)$ as

$$\boldsymbol{A}(t) = \partial\boldsymbol{y}(t)/\partial\boldsymbol{a}, \tag{2.21a}$$

$$\boldsymbol{B}(t) = \partial\boldsymbol{p}(t)/\partial\boldsymbol{a}. \tag{2.21b}$$

The variational equations are

$$\dot{\boldsymbol{A}} = \bar{\boldsymbol{p}}\,\nabla c^T\boldsymbol{A} + (c/|\boldsymbol{p}|)\,\boldsymbol{P}_\perp\boldsymbol{B} \tag{2.22a}$$

$$\dot{\boldsymbol{B}} = -|\boldsymbol{p}|\,(\nabla\nabla c)\,\boldsymbol{A} - \nabla c\bar{\boldsymbol{p}}^T\boldsymbol{B}. \tag{2.22b}$$

The equation for $\boldsymbol{A}$ is identical to (2.18) because by previous definition $|\boldsymbol{p}| = 1/c$ and

$$\begin{aligned}\boldsymbol{M} &= \frac{\partial\boldsymbol{p}(t)}{\partial\boldsymbol{a}}\left[\frac{\partial\boldsymbol{y}(t)}{\partial\boldsymbol{a}}\right]^{-1} \\ &= \boldsymbol{B}\boldsymbol{A}^{-1}\end{aligned} \tag{2.23}$$

independent of the particular choice of $\boldsymbol{a}$, as long as the inverse of $\boldsymbol{A}$ exists. It is clear from (2.21a) that $\boldsymbol{A}$ represents the mapping $\boldsymbol{a}\to\boldsymbol{y}(t)$. If $\boldsymbol{a}$ is specified as $\boldsymbol{y}(t_0)$, then det ($\boldsymbol{A}$) is the jacobian of the mapping from the initial to the current position. Also, (2.20) then has the familiar form of ray theory, i.e. the ray amplitude goes as the inverse square root of the jacobian of the mapping.

An equation similar to (2.19) can be obtained from (2.22*b*). Direct integration of this equation gives

$$\det \boldsymbol{B}(t) = \det \boldsymbol{B}(t_0)\frac{c(\boldsymbol{y}(t_0))}{c(\boldsymbol{y}(t))}\exp\left[-\int_{t_0}^{t}\frac{\mathrm{d}t}{c(t)}\operatorname{tr}\nabla\nabla c\cdot\boldsymbol{M}^{-1}(t)\right]. \tag{2.24}$$

Because det ($\boldsymbol{A}$) = det ($\boldsymbol{B}$)/det ($\boldsymbol{M}$), (2.24) implies that the amplitude V of (2.20) depends only upon the matrix $\boldsymbol{M}$, a fact also apparent from (2.17). This means that in calculating the solution $u(\boldsymbol{x}, t)$, one does not need $\boldsymbol{A}$ and $\boldsymbol{B}$ individually, but only in the combination $\boldsymbol{M} = \boldsymbol{B}\boldsymbol{A}^{-1}$. In fact, it will be shown in §3 that the magnitude $|V|$ of the amplitude V depends only upon the imaginary part of $\boldsymbol{M}(t)$, and in §4 that V depends only upon a well defined subset of $\boldsymbol{M}$.

2.4. *The paraxial approximation: gaussian wave packets*

To summarize the results of this section, the phase $\phi(\boldsymbol{x}, t)$ remains constant along the ray $\boldsymbol{x} = \boldsymbol{y}(t)$. The ray equations for $\boldsymbol{y}$ and tangent vector $\bar{\boldsymbol{p}}$ are given in (2.9). The matrix $\boldsymbol{M}$ defined in (2.16) is related to $\boldsymbol{A}$ and $\boldsymbol{B}$, which satisfy

$$\dot{\boldsymbol{A}} = \boldsymbol{T}\boldsymbol{A} + c^2\boldsymbol{P}_{\perp}\boldsymbol{B}, \tag{2.25a}$$

$$\dot{\boldsymbol{B}} = -(1/c)\,\nabla\nabla c\boldsymbol{A} - \boldsymbol{T}^T\boldsymbol{B}, \tag{2.25b}$$

with initial conditions

$$\boldsymbol{A}(t_0) = \boldsymbol{A}_0, \tag{2.25c}$$

$$\boldsymbol{B}(t_0) = \boldsymbol{B}_0, \tag{2.25d}$$

In (2.25*a*) and (2.25*b*),

$$\boldsymbol{T} = \bar{\boldsymbol{p}}\nabla c^T. \tag{2.26}$$

The equation for $\boldsymbol{M}$ is therefore

$$\dot{\boldsymbol{M}} = -(1/c)\,\nabla\nabla c - c^2\boldsymbol{M}\boldsymbol{P}_{\perp}\boldsymbol{M} - \boldsymbol{M}\boldsymbol{T} - \boldsymbol{T}^T\boldsymbol{M}, \tag{2.27a}$$

with initial condition

$$\begin{aligned}\boldsymbol{M}(t_0) &= \boldsymbol{B}_0\boldsymbol{A}_0^{-1}\\ &= \boldsymbol{M}_0.\end{aligned} \tag{2.27b}$$

The matrix $\boldsymbol{M}$ satisfies a nonlinear Ricatti equation that can be linearized through the introduction of the intermediate matrices $\boldsymbol{A}$ and $\boldsymbol{B}$. Equation (2.27*a*) is a generalization of the so-called 'aktinal' equation (Thomson & Chapman 1985). The term aktinal is derived from the Greek aktis, meaning a beam of light.

We are now in the position to expand $\phi(\boldsymbol{x}, t)$ about the ray position $\boldsymbol{y}(t)$,

$$\phi(\boldsymbol{x}, t) = \phi(\boldsymbol{y}, t) + \nabla\phi(\boldsymbol{y}, t)\cdot(\boldsymbol{x}-\boldsymbol{y}) + \tfrac{1}{2}(\boldsymbol{x}-\boldsymbol{y})\cdot\nabla\nabla\phi(\boldsymbol{y}, t)\cdot(\boldsymbol{x}-\boldsymbol{y}) + \dots. \tag{2.28}$$

From the previous results, it follows that $\phi(\boldsymbol{y}(t), t) = \phi_0$, a constant. The paraxial approximation follows from (2.28) by retaining terms up to and including quadratic.

In this approximation,

$$\phi(\boldsymbol{x},t) = \phi_0+\boldsymbol{p}(t)\cdot(\boldsymbol{x}-\boldsymbol{y}(t))+\tfrac{1}{2}(\boldsymbol{x}-\boldsymbol{y}(t))\cdot\boldsymbol{M}(t)\cdot(\boldsymbol{x}-\boldsymbol{y}(t)). \tag{2.29}$$

We now specify the ray $\boldsymbol{y}(t)$ to be in real space, i.e. a real ray. Then $\boldsymbol{y}_0$ and $\boldsymbol{p}_0$ must be real vectors. The ray equations (2.9) then guarantee that the ray remains in real space for $t > t_0$. However, the matrix $\boldsymbol{M}_0$ is not real, and we assume that $\mathrm{Im}\,(\boldsymbol{M}_0)$ is positive definite. It is shown in Appendix B that this condition ensures that $\mathrm{Im}\,(\boldsymbol{M})$ remains positive definite. Finally, the asymptotic solutions (2.2), (2.20) and (2.29) with these specifications forms what we call a gaussian wave packet.

3. Some general results

3.1. *Energy conservation and properties of $\boldsymbol{A}$ and $\boldsymbol{M}$*

The complex matrix $\boldsymbol{M}$ is the matrix of second derivatives of ϕ. In particular, $\boldsymbol{M}$ must be symmetric. It is established in Appendix B that (2.27) generates a symmetric $\boldsymbol{M}(t)$ if the initial $\boldsymbol{M}_0$ is symmetric. There it is also shown that the imaginary part of $\boldsymbol{M}(t)$ is positive definite, as it should be for a GWP. These results follow from the evolution equations (2.9) and (2.25). The proofs rely upon the fact that the matrices $\boldsymbol{P}_\perp$ and $\nabla\nabla c$ in (2.25) are real and symmetric, and that $\boldsymbol{T}$ is real. It is also shown in Appendix B that $\boldsymbol{A}$ is nonsingular. Therefore $\boldsymbol{A}^{-1}$ exists, and (2.20) shows that the amplitude V remains bounded everywhere in real space. In particular, there are no unphysical singularities at the geometrical caustics and foci of real rays. The only restrictions on the initial conditions are that (1) $\boldsymbol{A}_0^{-1}$ exists, (2) that $\boldsymbol{M}_0$ is symmetric and, (3) that $\mathrm{Im}\,(\boldsymbol{M}_0)$ is positive definite, all of which are essential from physical requirements on the initial wave packet.

It follows from (B 7) of Appendix B that

$$|\det \boldsymbol{A}(t)| = |\det \boldsymbol{A}_0|\left[\frac{\det \mathrm{Im}\,(\boldsymbol{M}_0)}{\det \mathrm{Im}\,(\boldsymbol{M}(t))}\right]^{\frac{1}{2}}. \tag{3.1}$$

The phase of $\det(\boldsymbol{A})$ follows from the imaginary part of (2.19)

$$\begin{aligned}\frac{\mathrm{d}}{\mathrm{d}t}\arg[\det(\boldsymbol{A})] &= \mathrm{tr}\,[(c^2\boldsymbol{P}_\perp\,\mathrm{Im}\,(\boldsymbol{M})] \\ &\geqslant 0,\end{aligned} \tag{3.2}$$

where the inequality follows from the positive definiteness of $\mathrm{Im}\,(\boldsymbol{M})$. Equations (2.20), (3.1) and (3.2) show that the amplitude V depends only upon $\mathrm{Im}\,\boldsymbol{M}$. Hence, the GWP is completely described by the complex matrix $\boldsymbol{M}$.

Equation (3.1) in combination with (2.2), (2.20) and (2.29) implies an energy-conservation result for GWPs in n dimensions, $n = 2$ or 3:

$$\int_{R^n}\rho(\boldsymbol{y}(t))\,|u(\boldsymbol{x},t)|^2\,\mathrm{d}\boldsymbol{x} = \left[\frac{2\pi}{\omega}\right]^{\frac{1}{2}n}\frac{\rho(\boldsymbol{y}_0)\,|V(t_0)|^2}{[\det \mathrm{Im}\,(\boldsymbol{M}_0)]^{\frac{1}{2}}}. \tag{3.3}$$

3.2. *Fundamental solutions*

The general solution to the system of ordinary differential equations (2.25) can be simply represented in terms of two linearly independent fundamental solutions.

Define $(\boldsymbol{A}_1, \boldsymbol{B}_1)$ as the solution of (2.25) with particular initial conditions

$$\boldsymbol{A}_1(t_0) = \boldsymbol{I}, \tag{3.4a}$$

$$\boldsymbol{B}_1(t_0) = 0, \tag{3.4b}$$

where $\boldsymbol{I}$ is the identity matrix. Similarly, let $(\boldsymbol{A}_2, \boldsymbol{B}_2)$ be the solution for the initial conditions

$$\boldsymbol{A}_2(t_0) = 0, \tag{3.5a}$$

$$\boldsymbol{B}_2(t_0) = \boldsymbol{I}. \tag{3.5b}$$

Then the general solution of (2.25) is

$$\boldsymbol{A}(t) = \boldsymbol{A}_1(t)\,\boldsymbol{A}_0 + \boldsymbol{A}_2(t)\,\boldsymbol{B}_0, \tag{3.6a}$$

$$\boldsymbol{B}(t) = \boldsymbol{B}_1(t)\,\boldsymbol{A}_0 + \boldsymbol{B}_2(t)\,\boldsymbol{B}_0, \tag{3.6b}$$

and the general solution of (2.27) is

$$\boldsymbol{M}(t) = [\boldsymbol{B}_1(t) + \boldsymbol{B}_2(t)\,\boldsymbol{M}_0]\,[\boldsymbol{A}_1(t) + \boldsymbol{A}_2(t)\,\boldsymbol{M}_0]^{-1}. \tag{3.7}$$

Two simple but very important special cases for which all the GWP parameters can be found are considered in the next two subsections.

3.3. *A constant-velocity medium*

This case is particularly simple. The fundamental solutions are $\boldsymbol{A}_1 = \boldsymbol{I}$, $\boldsymbol{B}_1 = 0$, $\boldsymbol{A}_2 = tc^2\boldsymbol{P}_\perp$ and $\boldsymbol{B}_2 = \boldsymbol{I}$. The matrix $\boldsymbol{M}$ becomes

$$\boldsymbol{M}(t) = \boldsymbol{M}_0[\boldsymbol{I} + tc^2\boldsymbol{P}_\perp\boldsymbol{M}_0]^{-1}, \tag{3.8}$$

where the projection matrix $\boldsymbol{P}_\perp$ is constant. The phase ϕ is given by (2.29) where $\boldsymbol{p}$ is a constant vector pointing in the direction of propagation. The amplitude V of (2.20) follows from (2.24), (3.8) and $\det(\boldsymbol{A}) = \det(\boldsymbol{B})/\det(\boldsymbol{M})$ as

$$V(t) = V(t_0)\left[\frac{\rho(\boldsymbol{y}(t_0))}{\rho(\boldsymbol{y}(t))}\right]^{\frac{1}{2}}[\det(\boldsymbol{I} + tc^2\boldsymbol{P}_\perp\boldsymbol{M}_0)]^{-\frac{1}{2}}. \tag{3.9}$$

3.4. *A one-dimensional smoothly varying medium*

Let $c = c(x)$ and $\mu = \mu(x)$, where x is the single spatial coordinate. Without loss of generality, let the GWP start at $x = 0$ with initial direction in the positive x-direction. The pulse centre is subsequently at $s(t)$, which follows from (2.6). The variables M, A and B are now scalar quantities. The equation for $M(t)$ follows from (2.27a),

$$\dot{M} = (1/c)\,c_{xx} - 2(\dot{c}/c)\,M, \tag{3.10}$$

where $c_x = \mathrm{d}c/\mathrm{d}x$, and $c_{xx} = \mathrm{d}^2c/\mathrm{d}x^2$. This can be solved to give

$$M = (c^2(0)/c^2(s))\,M_0 + [c_x(0) - c_x(s)]/c^2(s). \tag{3.11}$$

Similarly, $A = c(s)\,A_0$, and B follows simply. Thus, (2.2), (2.20) and (2.29) give the solution

$$u = V(0)\left[\frac{\rho(0)\,c(0)}{\rho(s)\,c(s)}\right]^{\frac{1}{2}} \exp\left(\mathrm{i}\omega\left[\frac{1}{c(s)}(x-s(t))+\frac{1}{2}\left[M_0+\frac{c_x(0)-c_x(s)}{c^2(0)}\right]\left[\frac{c(0)}{c(s)}(x-s(t))\right]^2\right]\right). \tag{3.12}$$

Note that the pulse width, $(\omega \operatorname{Im} M)^{-\frac{1}{2}}$, goes as $c(s)/c(0)$, and so it takes the same amount of time to pass a given point.

4. Dynamic ray-tracing coordinates

It turns out to be very helpful to define a moving coordinate frame relative to the packet centre $\boldsymbol{y}(t)$. This system of coordinates has been described by Popov & Psencik (1978) and Hubral (1980). A brief review follows. Let $\boldsymbol{n}(t)$ and $\boldsymbol{b}(t)$ be the usual normal and binormal unit vectors that satisfy the Frenet equations

$$\frac{1}{c}\dot{\boldsymbol{p}} = \kappa\boldsymbol{n}, \tag{4.1a}$$

$$\frac{1}{c}\dot{\boldsymbol{n}} = -\kappa\overline{\boldsymbol{p}}+\tau\boldsymbol{b}, \tag{4.1b}$$

$$\frac{1}{c}\dot{\boldsymbol{b}} = -\tau\boldsymbol{n}. \tag{4.1c}$$

Here κ is the ray curvature, and τ the ray torsion. The radius of curvature of the ray is $\rho = 1/\kappa$. Define the angle

$$\epsilon(t) = \epsilon_0+\int_{t_0}^{t}\tau(t)\,c(\boldsymbol{y}(t))\,\mathrm{d}t, \tag{4.2}$$

where ϵ_0 is arbitrary, and also define the unit vectors $\boldsymbol{e}_j, j = 1,2,3$ as

$$\boldsymbol{e}_1(t) = \cos\epsilon(t)\,\boldsymbol{n}(t)-\sin\epsilon(t)\,\boldsymbol{b}(t), \tag{4.3a}$$

$$\boldsymbol{e}_2(t) = \sin\epsilon(t)\,\boldsymbol{n}(t)+\cos\epsilon(t)\,\boldsymbol{b}(t), \tag{4.3b}$$

$$\boldsymbol{e}_3(t) = \overline{\boldsymbol{p}}(t). \tag{4.3c}$$

Let $\boldsymbol{P}(t)$ be the matrix with vector $\boldsymbol{e}_j$ in column $j, j = 1,3$. The following equation then summarizes (4.1)–(4.3)

$$\dot{\boldsymbol{P}}(t) = \boldsymbol{P}(t)\,\boldsymbol{N}(t), \tag{4.4}$$

where

$$\boldsymbol{N}(t) = c\kappa\begin{bmatrix} 0 & 0 & \cos\epsilon \\ 0 & 0 & \sin\epsilon \\ -\cos\epsilon & -\sin\epsilon & 0 \end{bmatrix}. \tag{4.5}$$

Note that $\boldsymbol{P}^{-1} = \boldsymbol{P}^T$ and $\boldsymbol{N}^T = -\boldsymbol{N}$.

So far no particular coordinate system has been specified for $\boldsymbol{A}$, $\boldsymbol{B}$ and $\boldsymbol{M}$. They are now defined relative to the dynamic ray-tracing system as $\overline{\boldsymbol{A}}$, $\overline{\boldsymbol{B}}$ and $\overline{\boldsymbol{M}}$, where

$$\overline{\boldsymbol{A}}(t) = \boldsymbol{P}^T(t)\,\boldsymbol{A}(t), \tag{4.6a}$$

$$\overline{\boldsymbol{B}}(t) = \boldsymbol{P}^T(t)\,\boldsymbol{B}(t), \tag{4.6b}$$

$$\overline{\boldsymbol{M}}(t) = \overline{\boldsymbol{B}}\overline{\boldsymbol{A}}^{-1}. \tag{4.6c}$$

The inverse of $\overline{\boldsymbol{M}}(t)$ is defined as

$$\begin{aligned}\overline{\boldsymbol{R}}(t) &= \overline{\boldsymbol{M}}(t)^{-1}\\ &= \overline{\boldsymbol{A}}\overline{\boldsymbol{B}}^{-1}.\end{aligned} \tag{4.7}$$

The evolution equations for $\overline{\boldsymbol{A}}$, $\overline{\boldsymbol{B}}$, $\overline{\boldsymbol{M}}$ and $\overline{\boldsymbol{R}}$ follow from (2.25), (2.27), (4.4) and (4.10) as

$$\dot{\overline{\boldsymbol{A}}}(t) = \boldsymbol{Q}\overline{\boldsymbol{A}}+c^2\overline{\boldsymbol{P}}_\perp\overline{\boldsymbol{B}}, \tag{4.8a}$$

$$\dot{\overline{\boldsymbol{B}}}(t) = (-1/c)\,\overline{\boldsymbol{C}}\overline{\boldsymbol{A}}-\boldsymbol{Q}^T\overline{\boldsymbol{B}}, \tag{4.8b}$$

$$\dot{\overline{\boldsymbol{R}}}(t) = (1/c)\,\overline{\boldsymbol{R}}\overline{\boldsymbol{C}}\overline{\boldsymbol{R}}+c^2\overline{\boldsymbol{P}}_\perp+\boldsymbol{Q}\overline{\boldsymbol{R}}+\overline{\boldsymbol{R}}\boldsymbol{Q}^T, \tag{4.8c}$$

$$\dot{\overline{\boldsymbol{M}}}(t) = (-1/c)\,\overline{\boldsymbol{C}}-c^2\overline{\boldsymbol{M}}\overline{\boldsymbol{P}}_\perp\overline{\boldsymbol{M}}-\overline{\boldsymbol{M}}\boldsymbol{Q}-\boldsymbol{Q}^T\overline{\boldsymbol{M}}, \tag{4.8d}$$

where

$$\begin{aligned}\boldsymbol{Q}(t) &= \boldsymbol{P}^T\dot{\boldsymbol{T}}\boldsymbol{P}-\boldsymbol{N}\\ &= \begin{bmatrix}0 & 0 & -c\kappa\cos\epsilon\\ 0 & 0 & -c\kappa\sin\epsilon\\ 0 & 0 & \dot{c}/c\end{bmatrix},\end{aligned} \tag{4.9a}$$

$$\begin{aligned}\overline{\boldsymbol{P}}_\perp(t) &= \boldsymbol{P}^T(t)\,\boldsymbol{P}_\perp(t)\,\boldsymbol{P}(t)\\ &= \begin{bmatrix}1 & 0 & 0\\ 0 & 1 & 0\\ 0 & 0 & 0\end{bmatrix},\end{aligned} \tag{4.9b}$$

$$\overline{\boldsymbol{C}}(t) = \boldsymbol{P}^T\nabla\nabla c\boldsymbol{P}^T. \tag{4.9c}$$

Note that $\boldsymbol{Q}\overline{\boldsymbol{P}}_\perp = \overline{\boldsymbol{P}}_\perp\boldsymbol{Q} = 0$. Equations (4.8) simplify considerably when $\overline{\boldsymbol{C}} = 0$. This specific case is considered in the next section. However, we note some general decoupling in the equation for $\overline{\boldsymbol{M}}$. Define the 2×2 submatrices

$$\overline{\boldsymbol{M}}_\perp = \overline{\boldsymbol{P}}_\perp\overline{\boldsymbol{M}}\overline{\boldsymbol{P}}_\perp, \tag{4.10a}$$

$$\overline{\boldsymbol{C}}_\perp = \overline{\boldsymbol{P}}_\perp\overline{\boldsymbol{C}}\overline{\boldsymbol{P}}_\perp, \tag{4.10b}$$

then (4.8d) implies an equation for $\overline{\boldsymbol{M}}_\perp$ that does not depend upon the outer elements $\overline{M}_{i3}, i = 1,2,3$.

$$\dot{\overline{\boldsymbol{M}}}_\perp = (-1/c)\,\overline{\boldsymbol{C}}_\perp-c^2\overline{\boldsymbol{M}}_\perp^2. \tag{4.11}$$

This equation is identical to the 'aktinal' equation (Thomson & Chapman 1985) that is usually encountered in standard gaussian beam theory. The two coupled linear ordinary differential equations for $\overline{M}_{13}$ and $\overline{M}_{23}$ then depend on $\overline{\boldsymbol{M}}_\perp$, but not on $\overline{M}_{33}$. The equation for $\overline{M}_{33}$ depends upon $\overline{M}_{13}$, $\overline{M}_{23}$, and $\overline{M}_{33}$, but not upon $\overline{\boldsymbol{M}}_\perp$ directly. The latter equation can be solved formally to yield

$$\overline{M}_{33}(t) = \frac{c^2(t_0)}{c^2}\overline{M}_{330}+\frac{1}{c^2}[\boldsymbol{e}_3(t_0)\cdot\nabla c(t_0)-\boldsymbol{e}_3\cdot\nabla c]+\frac{1}{c^2}\int_{t_0}^{t}F(t)\,\mathrm{d}t, \tag{4.12}$$

where $c(t) = c(\boldsymbol{y}(t))$, and

$$F(t) = 2c^3\kappa(\overline{M}_{13}\cos\epsilon+\overline{M}_{23}\sin\epsilon)-c^4(\overline{M}_{13}^2+\overline{M}_{23}^2). \tag{4.13}$$

The final term on the right-hand side of (4.12) depends upon the 13 and 23 elements of $\overline{\boldsymbol{M}}$, and these in turn depend upon the transverse submatrix $\boldsymbol{M}_{\perp}$. If this coupling is small, one can approximate

$$\overline{M}_{33}(t) = \frac{c^2(t_0)}{c^2}\overline{M}_{330} + \frac{1}{c^2}[\boldsymbol{e}_3(t_0)\cdot\nabla c(t_0) - \boldsymbol{e}_3\cdot\nabla c], \tag{4.14}$$

which is identical with the one-dimensional result (3.11). This means that the length of the pulse in the direction of propagation increases (decreases) as the GWP moves into regions of higher (lower) wave speed.

The 2×2 submatrix $\overline{\boldsymbol{M}}_{\perp}$ corresponds to the usual wavefront curvature matrix of ordinary ray theory. It can be shown that the amplitude V of the GWP depends only on this matrix, and not on the elements $\overline{M}_{i3}$, $i = 1, 2, 3$. Thus, from (4.8a) and (4.10a)

$$\begin{aligned}\frac{\mathrm{d}}{\mathrm{d}t}\lg(\det\overline{\boldsymbol{A}}) &= \operatorname{tr}\dot{\overline{\boldsymbol{A}}}\overline{\boldsymbol{A}}^{-1}\\ &= (\dot{c}/c) + c^2\operatorname{tr}\overline{\boldsymbol{M}}_{\perp},\end{aligned} \tag{4.15}$$

where $\operatorname{tr}\overline{\boldsymbol{M}}_{\perp} = \overline{M}_{11} + \overline{M}_{22}$. Integrating (4.15) gives

$$\frac{\det\boldsymbol{A}}{\det\boldsymbol{A}_0} = c\exp\int_{t_0}^{t} c^2\operatorname{tr}\overline{\boldsymbol{M}}_{\perp}\,\mathrm{d}t. \tag{4.16}$$

The result for V then follows from (2.20).

5. Media with constant velocity gradients

5.1. *Ray parameters*

Media in which the gradient of the velocity is constant, i.e. $\nabla\nabla c = 0$, are particularly interesting. It is known (Michaels 1977; Hubral 1980) that the rays in these media are circular arcs with zero torsion. In general, one can obtain closed-form solutions for the ray tube area and associated ray parameters. In this section, the GWP equations are considered for the case of $\nabla c = \text{const.}$, and solved for arbitrary initial data.

Let the velocity in the medium be

$$c(\boldsymbol{x}) = c_0 + \nabla c\cdot\boldsymbol{x}, \tag{5.1}$$

where $\nabla c = \text{const.}$ Of course, the medium cannot be infinite in extent, because negative values of $c(\boldsymbol{x})$ are not allowed. Consider a ray that starts at $\boldsymbol{x} = \boldsymbol{y}_0$ at $t = t_0$ with initial ray direction $\boldsymbol{e}_3(t_0)$. We will use both t and the arc length parameter $s(t)$ of (2.6) as ray parameters. For example, we will write

$$c(s) = c(\boldsymbol{y}(t)). \tag{5.2}$$

The initial value of s at $t = t_0$ is $s = s_0$. For $t > t_0$, the ray describes a circular arc in the plane of $\boldsymbol{e}_3(t_0)$ and $\nabla\phi$, see figure 1. Let the vector $\boldsymbol{e}_2$ be orthogonal to this plane initially. This is the same as taking ϵ_0 of (4.2) equal to zero. Because the ray has no torsion it follows that $\boldsymbol{e}_2(t)$ remains constant along the ray. The vector $\boldsymbol{e}_1(t_0)$ is in the plane of $\boldsymbol{e}_3(t_0)$ and $\nabla\phi$ with positive component in the direction of $-\nabla\phi$.

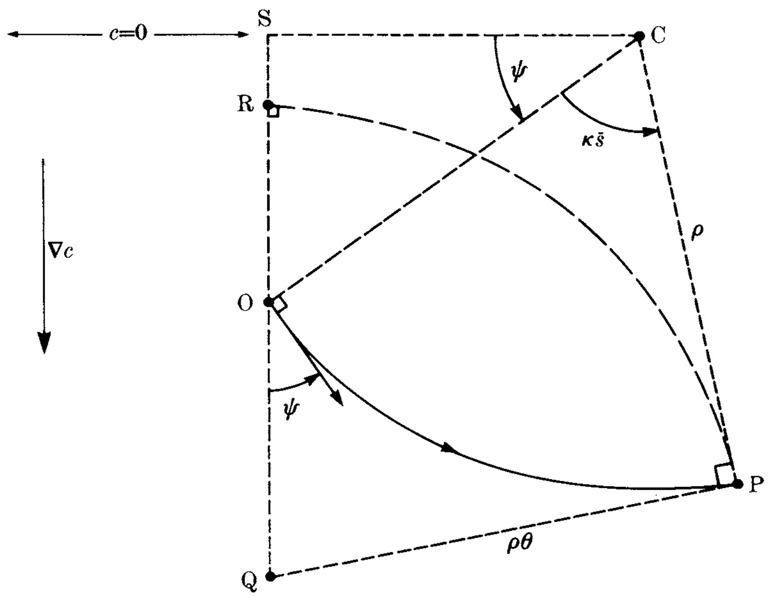

FIGURE 1. The ray parameters for a constant velocity gradient medium. O is the ray position at t_0, P the ray position at t. The length $|\mathrm{SQ}| = |\mathrm{SO}| \cosh [|\nabla c|\,(t-t_0)]$ determines P.

The centre of the circular ray path is the point $\boldsymbol{y}_c$ where the line through $\boldsymbol{y}_0$ in the direction $\boldsymbol{e}_1(t_0)$ intersects the plane $c(\boldsymbol{x}) = 0$. The distance from $\boldsymbol{y}_c$ to $\boldsymbol{y}_0$ is the radius of curvature ρ, which is constant. We will also use the curvature $\kappa = 1/\rho$. It is useful to introduce the angle ψ between $\boldsymbol{e}_3(t_0)$ and ∇c. Thus, $0 < \psi < \pi$, and

$$\cos\psi = \boldsymbol{e}_3(t_0)\cdot(\nabla c/|\nabla c|). \tag{5.3}$$

The above results can be written succinctly as

$$\kappa = \frac{1}{\rho} = \frac{|\nabla c|}{c(s_0)}\sin\psi, \tag{5.4a}$$

$$\boldsymbol{e}_1(t_0) = \cot\psi\,\boldsymbol{e}_3(t_0) - \operatorname{cosec}\psi(\nabla c/|\nabla c|), \tag{5.4b}$$

$$\boldsymbol{y}_c = \boldsymbol{y}_0 + \rho\boldsymbol{e}_1(t_0). \tag{5.4c}$$

The subsequent ray vectors are

$$\boldsymbol{y}(t) = \boldsymbol{y}_c - \rho\boldsymbol{e}_1(t), \tag{5.5a}$$

$$\boldsymbol{e}_1(t) = \cos\kappa\bar{s}\,\boldsymbol{e}_1(t_0) - \sin\kappa\bar{s}\,\boldsymbol{e}_3(t_0), \tag{5.5b}$$

$$\boldsymbol{e}_3(t) = \sin\kappa\bar{s}\,\boldsymbol{e}_1(t_0) + \cos\kappa\bar{s}\,\boldsymbol{e}_3(t_0), \tag{5.5c}$$

where

$$\bar{s} = s - s_0. \tag{5.6}$$

The wave speed along the ray is

$$c(s) = c(s_0)\operatorname{cosec}\psi\,\sin(\psi + \kappa\bar{s}). \tag{5.7}$$

This equation is readily apparent from figure 1 by noting that $(1/c)\sin(\psi+\kappa\bar{s})$, the slowness component perpendicular to ∇c, is conserved along a ray. The previous equations are simpler than the analogous ones in Hubral (1980). Note that $\frac{1}{2}\pi-\psi$ is the same as Hubral's angle u. The variable d in Hubral (1980) is actually equal to zero. The relation between t and s follows from (2.6) and (5.7) as

$$t-t_0 = \frac{1}{|\nabla c|}\lg[\cot\tfrac{1}{2}(\psi)\tan\tfrac{1}{2}(\psi+\kappa\bar{s})], \tag{5.8a}$$

$$s-s_0 = \rho[2\arctan(\tan\tfrac{1}{2}(\psi)\,\mathrm{e}^{|\nabla c|(t-t_0)})-\psi]. \tag{5.8b}$$

Also define for later use,

$$\begin{aligned} c^{(1)}(s) &= \int_{s_0}^{s} c(s)\,\mathrm{d}s \\ &= \rho c(s_0)\operatorname{cosec}\psi[\cos\psi-\cos(\psi+\kappa\bar{s})], \end{aligned} \tag{5.9}$$

and

$$\begin{aligned} \theta(s) &= \kappa\frac{c^{(1)}(s)}{c(s)} \\ &= \operatorname{cosec}(\psi+\kappa\bar{s})[\cos\psi-\cos(\psi+\kappa\bar{s})] \\ &= \sin\psi\sinh[|\nabla c|(t-t_0)]. \end{aligned} \tag{5.10}$$

The latter result is a consequence of (5.8a) and (5.9).

5.2. *Solution of the* GWP *parameters*

First consider the matrix $\bar{\boldsymbol{R}}$. Equation (4.8c) is linear in $\bar{\boldsymbol{R}}$. Therefore, by comparison with the solution for a constant velocity medium, we consider a solution of the form

$$\bar{\boldsymbol{R}}(t) = \boldsymbol{X}^T(t)\,\bar{\boldsymbol{R}}_0\,\boldsymbol{X}(t)+c^{(1)}(s)\,\bar{\boldsymbol{P}}_\perp, \tag{5.11}$$

with initial condition $\boldsymbol{X}(t_0)=\boldsymbol{I}$, the identity matrix. Substituting (5.11) into (4.8c), gives the following equation for $\boldsymbol{X}(t)$

$$\dot{\boldsymbol{X}} = \boldsymbol{X}\boldsymbol{Q}^T. \tag{5.12}$$

The matrix $\boldsymbol{Q}$ is given by (4.9a) with $\epsilon=0$. Solving (5.12) gives

$$\boldsymbol{X}(t) = \begin{bmatrix} 1 & 0 & 0 \\ 0 & 1 & 0 \\ -\theta\dfrac{c(s)}{c(s_0)} & 0 & \dfrac{c(s)}{c(s_0)} \end{bmatrix}. \tag{5.13}$$

Note that $\boldsymbol{X}$ is a real matrix that reduces to the identity matrix for a homogeneous medium. Also, from (5.11) and (5.13),

$$\bar{\boldsymbol{R}} = \boldsymbol{X}^T[\bar{\boldsymbol{R}}_0+c^{(1)}(s)\,\bar{\boldsymbol{P}}_\perp]\,\boldsymbol{X}, \tag{5.14}$$

so that, by (4.7)

$$\bar{\boldsymbol{M}}(t) = \boldsymbol{X}^{-1}(t)\,\bar{\boldsymbol{M}}_0[\boldsymbol{I}+c^{(1)}(s)\,\bar{\boldsymbol{P}}_\perp\bar{\boldsymbol{M}}_0]^{-1}\boldsymbol{X}^{-1T}(t), \tag{5.15}$$

where
$$\boldsymbol{X}^{-1}(t) = \begin{bmatrix} 1 & 0 & 0 \\ 0 & 1 & 0 \\ \theta(s) & 0 & \dfrac{c(s_0)}{c(s)} \end{bmatrix}. \tag{5.16}$$

Thus, $\boldsymbol{M}$ resembles closely the solution for the homogeneous medium, see (3.8).

The amplitude $V(t)$ in (2.20) depends upon $\det[\boldsymbol{A}(t)]$. However, $\det(\boldsymbol{A}) = \det(\overline{\boldsymbol{R}})\det(\boldsymbol{B})$, and $\det(\boldsymbol{B})$ follows from (2.24). Therefore, the amplitude is

$$V(t) = V(t_0)\left[\frac{\rho(s_0)\,c(s_0)}{\rho(s)\,c(s)}\right]^{\frac{1}{2}}[\det(\boldsymbol{I}+c^{(1)}(s)\,\overline{\boldsymbol{P}}_{\perp}\overline{\boldsymbol{M}}_0)]^{-\frac{1}{2}}. \tag{5.17}$$

This should be compared with the homogeneous result in (3.9). Finally, note that the matrices $\overline{\boldsymbol{A}}(t)$ and $\overline{\boldsymbol{B}}(t)$ defined in (4.6) can be obtained explicitly from (4.8) as

$$\overline{\boldsymbol{A}} = \boldsymbol{X}^T\overline{\boldsymbol{A}}_0 + c^{(1)}\overline{\boldsymbol{P}}_{\perp}\overline{\boldsymbol{B}}_0, \tag{5.18a}$$

$$\overline{\boldsymbol{B}} = \boldsymbol{X}^{-1}\overline{\boldsymbol{B}}_0. \tag{5.18b}$$

5.3. *Plane waves and point sources*

Consider, for example, an initial GWP that has a plane wavefront, i.e. $\overline{\boldsymbol{M}}_{\perp 0} = 0$, where $\overline{\boldsymbol{M}}_{\perp}$ is defined in (4.10*a*). Let us also assume that the pulse is initially oriented perpendicular to the wavefront, i.e. $\overline{\boldsymbol{M}}_0 = \mathrm{diag}(0, 0, \overline{M}_{330})$. Then at later times, $\overline{\boldsymbol{M}} = \mathrm{diag}(0, 0, \overline{M}_{33})$ where $\overline{M}_{33} = \overline{M}_{330}[c(s_0)/c(s)]^2$. Thus, a plane GWP remains plane, and the pulse length changes as the velocity changes. As c increases the pulse length increases, and conversely, as c decreases the pulse length decreases.

In the opposite limit from a plane wave, consider an initial pulse with zero wavefront curvature, i.e. $\overline{\boldsymbol{R}}_0 = \mathrm{diag}(0, 0, 1/\overline{M}_{330})$. In ordinary ray theory, this initial condition defines a point source. The GWP solution follows from (5.11) and (5.13) as $\overline{\boldsymbol{M}} = \mathrm{diag}(1/c^{(1)}(s), 1/c^{(1)}(s), \overline{M}_{33})$, where again $\overline{M}_{33} = \overline{M}_{330}[c(s_0)/c(s)]^2$. The current wavefront curvature is given by the submatrix $\overline{\boldsymbol{M}}_{\perp}$, which in this case is just $\mathrm{diag}(1/c^{(1)}(s), 1/c^{(1)}(s))$, and the magnitude of the vector $\boldsymbol{p}$, which is $1/c$, by definition. Thus, the wavefront curvature is $c(s)/c^{(1)}(s)$. Alternatively, the wavefront of the point source has a radius of curvature equal to $\rho\theta(s)$, where ρ is the radius of curvature of the ray, and $\theta(s)$ is defined in (5.10).

Note from (5.4) and (5.10) that the radius of curvature for the point source can be written as

$$\rho\theta(s) = (c(s_0)/|\nabla c|)\sinh[|\nabla c|\,(t-t_0)]. \tag{5.19}$$

If the source point is O in figure 1, then the centre of curvature of the wavefront is at the point Q. In fact, at time t, the entire wavefront from a point source at O is given by the circle of radius $\rho\theta$ about Q. This suggests an easy geometrical procedure, with ruler and compass, to determine the ray position P at any time t given the initial position O and the initial direction ψ. First, construct the right-angle triangle OSC such that $|\mathrm{OS}| = |\mathrm{OC}|\sin\psi$ and S, Q lie on the line $c = 0$. Then draw the circle of radius $|\mathrm{OC}|$ about C. Next, find the point Q such that SOQ is a straight line and $|\mathrm{SQ}|/|\mathrm{SO}| = \cosh[|\nabla c|\,(t-t_0)]$. Then draw the tangent to the circle that passes through Q. The point of tangency is P. Note that the wavefront surface RP at time t due to the point source at O is the circle of radius $|\mathrm{QP}|$ about Q.

5.4. *Arbitrary initial data*

Next consider more-general initial conditions for the GWP. Specifically, let us consider the general case of $\overline{M}_0$ diagonal, $\overline{M}_0 = \mathrm{diag}\,(m_{10}, m_{20}, m_{30})$, m_{i0} complex, $\mathrm{Im}\,(m_{i0}) > 0, i = 1,2,3$. This GWP initially has its principal directions directed along the axes $e_j(t_0), j = 1,2,3$. For $t \geqslant t_0$, it follows from (5.13) and (5.15) that

$$\overline{M}(t) = \begin{bmatrix} m_1 & 0 & \theta m_1 \\ 0 & m_2 & 0 \\ \theta m_1 & 0 & m_3 \end{bmatrix}, \tag{5.20a}$$

where
$$m_j = \frac{m_{j0}}{1+c^{(1)}(s)\, m_{j0}}, \quad j = 1,2, \tag{5.20b}$$

$$m_3 = \frac{c(s_0)^2}{c(s)^2} m_{30} + \theta^2 m_1. \tag{5.20c}$$

The principal directions of the GWP therefore rotate relative to the ray vectors $e_j(t_0), j = 1,2,3$. Let the new principal directions of $\overline{M}$ be parallel to $v_j(t), j = 1,2,3$, where $v_j(t_0) = e_j(t_0)$. Thus, $v_2(t) = e_2(t_0)$, and

$$v_1(t) = \frac{1}{(1+\gamma^2(t))^{\frac{1}{2}}}[e_1(t)+\gamma(t)\, e_3(t)], \tag{5.21a}$$

$$v_3(t) = \frac{1}{(1+\gamma^2(t))^{\frac{1}{2}}}[-\gamma(t)\, e_1(t)+e_3(t)], \tag{5.21b}$$

where
$$\gamma(t) = \left(\frac{m_1-m_3}{2\theta m_1}\right)\left[\left[1+\left(\frac{2\theta m_1}{m_1-m_3}\right)^2\right]^{\frac{1}{2}}-1\right]. \tag{5.22}$$

Note that $v_1(t)$ and $v_3(t)$ are complex vectors. They are the eigenvectors of $\overline{M}$, but not of $\mathrm{Im}\,(\overline{M})$. The latter are the principal directions of the GWP. They are given by (5.21) and (5.22) with m_1 and m_3 replaced by $\mathrm{Im}\,(m_1)$ and $\mathrm{Im}\,(m_3)$, respectively. The eigenvalues of $\overline{M}$ are $\lambda_2(t) = m_2(t)$, and $\lambda_1(t)$ and $\lambda_3(t)$,

$$\begin{bmatrix} \lambda_1 \\ \lambda_3 \end{bmatrix} = \begin{bmatrix} m_1 \\ m_3 \end{bmatrix} \pm \theta m_1 \gamma. \tag{5.23}$$

Similarly, the eigenvalues of $\mathrm{Im}\,(\overline{M})$, and hence the principal widths of the GWP, are $\mathrm{Im}\,(m_2)$, and the other two follow from (5.22) and (5.23) with m_1 and m_3 replaced by $\mathrm{Im}\,(m_1)$ and $\mathrm{Im}\,(m_3)$, respectively.

Now consider the case when the arc length $\bar{s} = s - s_0$ is small relative to the radius of curvature of the ray, $\rho = 1/\kappa$. From the definition of $\theta(s)$ in (5.10), it follows that $\theta(s) = \kappa\bar{s} + O[(\kappa\bar{s})^2]$. Therefore, θ is approximately equal to the angle subtended by the arc from s_0 to $s(t)$. Expanding the eigenvalues for $\theta \ll 1$, gives

$$\lambda_1 = m_1 + \theta^2 \frac{m_1^2}{m_1 - m_3} + O(\theta^4), \tag{5.24a}$$

$$\lambda_3 = m_3 - \theta^2 \frac{m_1^2}{m_1 - m_3} + O(\theta^4). \tag{5.24b}$$

The eigenvectors $\boldsymbol{v}_1$ and $\boldsymbol{v}_3$ become

$$\boldsymbol{v}_1 = \boldsymbol{e}_1 + \theta(s)\frac{m_{10}}{m_{10}-m_{30}}\boldsymbol{e}_3(t) + O(\theta^2), \tag{5.25a}$$

$$\boldsymbol{v}_3 = \boldsymbol{e}_3 - \theta(s)\frac{m_{10}}{m_{10}-m_{30}}\boldsymbol{e}_1(t) + O(\theta^2). \tag{5.25b}$$

Consider the two limits of m_{10} and m_{30} both imaginary, and (1) $\mathrm{Im}\,(m_{10}) \gg \mathrm{Im}\,(m_{30})$ and (2) $\mathrm{Im}\,(m_{30}) \gg \mathrm{Im}\,(m_{10})$. Case (1) represents an initial GWP that is long in the direction of propagation and narrow in the orthogonal direction. If (1) corresponds to an initial GWP that is long and narrow, then (2) corresponds to one that is short and broad. Note that in either case it is not necessary to consider the width in the out-of-plane direction $\boldsymbol{e}_2$, because there is no coupling with the in-plane parameters because of the initial condition that $\overline{\boldsymbol{M}}_0$ is diagonal.

Case (1). The initial GWP can be visualized as a javelin-shaped disturbance propagating in the direction of it's axis. As it propagates, the centre of the GWP describes a circular arc of radius ρ. However, from (5.5) and (5.25) it is clear that to first order in θ, the principal directions $\boldsymbol{v}_1$ and $\boldsymbol{v}_3$ of $\boldsymbol{M}(t)$ remain real and equal to the initial principal directions $\boldsymbol{e}_1(t_0)$ and $\boldsymbol{e}_3(t_0)$. Therefore, the 'javelin' tends to maintain its initial orientation, even though it is not propagating in a straight line.

Case (2). In this case, the initial GWP may be considered as a discus perpendicular to the initial direction of propagation. As it propagates, the principal directions tend to follow the ray directions $\boldsymbol{e}_1(t)$ and $\boldsymbol{e}_3(t)$. There is no conservation-of-direction effect as for the javelin.

These apparently unusual wave-field events can be easily understood by simple geometrical arguments. Consider the discus event first. Figure 2 shows three points

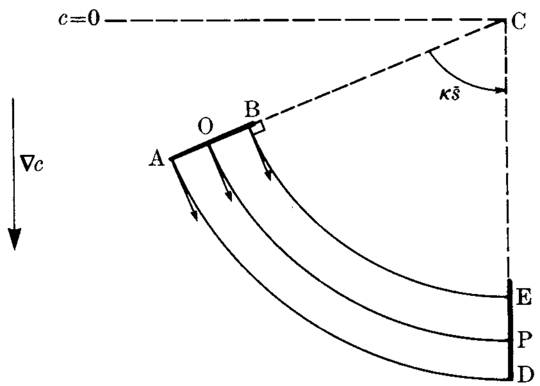

FIGURE 2. The ray picture for three points in a thin, flat GWP: the discus event.

A, B and O of the GWP at time t_0. As discussed before, the point O of the GWP is transported along the circular arc OP of radius |OC| arriving at P at time t. The angle subtended by the arc is $\kappa\bar{s} = (s-s_0)/\rho$, given by (5.8$b$). Now consider the ray path of point A. Its initial direction is the same as for O, therefore, the centre of curvature of the ray path is also at C. However, the radius of curvature is |AC|.

The point A is thus transported along a concentric arc to the point D. The angle subtended by the ray through A at time t is the same as that of the ray through O, by (5.8*b*). A similar argument holds for the ray through B. Hence, the discus AOB is transported as shown in figure 2 to DPE.

The case of the long, narrow GWP can be understood by considering figure 3. The centres of curvature of the ray paths through two points A and B on the GWP are now at C′ and C″, respectively. The radius of curvature of the ray path through A, for example, follows simply as $|AC'| = |OC| + |OA| \cot\psi$. The point A is transported at time t to the point D, with vector position $\boldsymbol{y}_D$. The latter follows from (5.5) as

$$\boldsymbol{y}_D = \boldsymbol{y}(t) + |OA|\,[(1 + \cot\psi\,\sin\kappa\bar{s})\,\boldsymbol{e}_3(t_0) + \cot\psi(1 - \cos\kappa\bar{s})\,\boldsymbol{e}_1(t_0)], \qquad (5.26)$$

where $\boldsymbol{y}(t)$ is the vector position of P. A similar equation follows for $\boldsymbol{y}_E$. The orientation and elongation of the GWP at time t follows from

$$\frac{\overrightarrow{ED}}{|AB|} = \boldsymbol{e}_3(t_0) + \cot\psi[\sin\kappa\bar{s}\boldsymbol{e}_3(t_0) + (1 - \cos\kappa\bar{s})\,\boldsymbol{e}_1(t_0)]. \qquad (5.27)$$

Hence, $|ED| > |AB|$. Also, the pulse rotates in the same sense as the ray direction (anticlockwise in figure 3) if $\psi < \frac{1}{2}\pi$, but in the opposite sense if $\psi > \frac{1}{2}\pi$. In either case, the rotation of the GWP is of order $(\kappa\bar{s})^2$, for small angle $\kappa\bar{s}$, in agreement with the findings above.

5.5. *Numerical illustrations*

A simulation of the 'discus', or flat GWP, is shown in figure 4. This figure displays four pictures of the envelope of the GWP at different times. The envelope, defined by taking the magnitude of the field $u(\boldsymbol{x}, t)$ times the phase factor $\exp[-\mathrm{i}\omega(\boldsymbol{x} - \boldsymbol{y})\cdot\boldsymbol{p}]$, is plotted for clarity. The circular ray trajectory is also shown for convenience. Note the behaviour is as predicted; the envelope rotates so as to remain perpendicular to the ray direction.

In both figures 4 and 5 the pulse initially propagates in a direction perpendicular to ∇c, and subsequently travels into regions of slower wave speed. It takes an infinite amount of time to reach the plane $c(\boldsymbol{x}) = 0$. Note that many of the pulse parameters simplify for the case of the initial pulse direction chosen ($\psi = \frac{1}{2}\pi$). Thus, $\rho = 1/|\nabla c|$, the angle $\kappa\bar{s} = (2t\rho)\arctan[\tanh(2t\rho)]$, the speed is $c(s) = \cos(\kappa\bar{s})$ and θ of (5.10) is $\theta = \tan\kappa\bar{s}$.

The opposite limit to the 'discus', the 'javelin' is shown in figure 5. The only difference between figures 4 and 5 is with the initial GWP parameters m_{10} and m_{30}. Note from figure 5 that the pulse maintains its orientation for a large ray angle $\kappa\bar{s}$. This is to be expected from (5.26) with $\cot\psi = 0$, as is the case here. In fact, note from the bottom pair of views in figure 5 that the ultimate sense of the pulse rotation is retrograde from that of the ray direction.

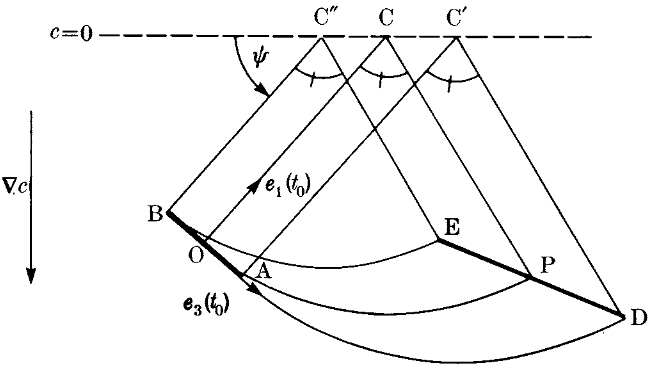

FIGURE 3. The ray picture for three points in a long, narrow GWP: the javelin event. Note that the three angles B C″ E, O C P and A C D are all equal $\kappa\bar{s}$.

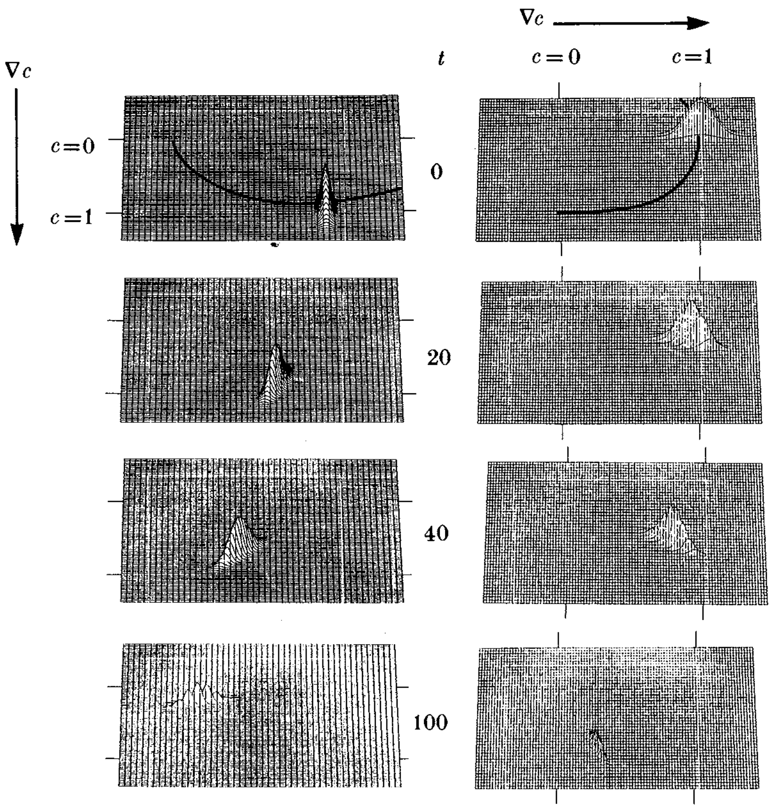

FIGURE 4. The flat 'discus' propagating in a medium of constant velocity gradient. The left and right series of pictures show two orthogonal perspectives of the envelope of the GWP at four times. The parameters are $\omega = 4, |\nabla c| = \frac{1}{50}, \psi = \frac{1}{2}\pi, m_{10} = \frac{1}{100}\mathrm{i}, m_{30} = \frac{1}{10}\mathrm{i}$. The top pair of views is at $t = 0$, and the subsequent pairs are at $t = 20, 40, 100$. The area shown is a square of side 100.

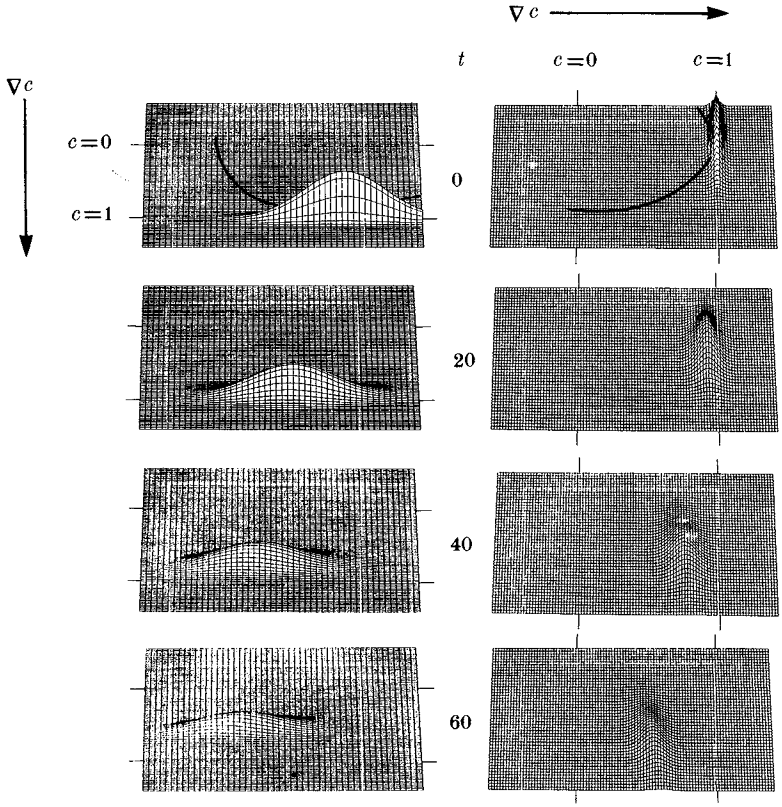

FIGURE 5. The case of a long, thin GWP in a medium of constant velocity gradient: the 'javelin'. The views are the same in figure 4, except that the bottom pair is for time $t = 60$. All other parameters are the same as figure 4, except the beam width and length parameters. Now we have $m_{10} = \frac{1}{10}\mathrm{i}$ and $m_{30} = \frac{1}{1000}\mathrm{i}$.

6. Reflection and transmission from curved interfaces

6.1. *Interface conditions*

Let $\bar{Z}(\xi_1, \xi_2) \in R^3$ be a surface across which the material parameters μ, ρ, suffer a discontinuity. We take ξ_1, ξ_2 to be orthogonal coordinates on the surface. Letting $\bar{Z}(0,0) = \bar{Z}_0$, we write the interface locally, near $\xi_1 = \xi_2 = 0$, as

$$\bar{Z}(\xi_1, \xi_2) = \bar{Z}_0 + \xi_1, \boldsymbol{t}_1 + \xi_2 \boldsymbol{t}_2 + (D_{11}\xi_1^2 + 2D_{12}\xi_1\xi_2 + D_{22}\xi_2^2)\boldsymbol{t}_3, \tag{6.1}$$

where $\boldsymbol{t}_1, \boldsymbol{t}_2$ are orthogonal unit vectors in the tangent plane at $\bar{Z}_0$, and $\boldsymbol{t}_3$ is the unit normal. The boundary conditions for u are

$$u \quad \text{continuous across} \quad \bar{Z}, \tag{6.2a}$$

$$\mu\nabla u \cdot \boldsymbol{t}_3 \quad \text{continuous across} \quad \bar{Z}. \tag{6.2b}$$

Now $\bar{Z}$ divides R^3 into two regions, Ω^-, and Ω^+. We consider a GWP of the standard form

$$U^{(I)} = V^{(I)}\,\mathrm{e}^{\mathrm{i}\omega\phi^{(I)}} \tag{6.3}$$

that is incident upon $\bar{Z}$ at $\bar{Z}_0$, from Ω^-. $U^{(I)}$ is the field u in the absence of an interface. We will represent the total field as

$$U = U^{(I)} + U^{(R)} \quad \text{for} \quad \boldsymbol{x} \in \Omega^-,$$
$$U = U^{(T)} \quad \text{for} \quad \boldsymbol{x} \in \Omega^+, \tag{6.4}$$

We show that (6.2) can be satisfied, asymptotically as $\omega \to \infty$ by taking $U^{(R)}$, $U^{(T)}$ to have the form of a GWP,

$$U^{(R)} = V^{(R)}\, \mathrm{e}^{\mathrm{i}\omega\phi^{(R)}},$$
$$U^{(T)} = V^{(T)}\, \mathrm{e}^{\mathrm{i}\omega\phi^{(T)}}. \tag{6.5}$$

Thus, from our previous theory, $\phi^{(R)}, \phi^{(T)}$ must satisfy the eikonal equation (2.7) in the appropriate regions, respectively, Ω^-, Ω^+. Each pulse will propagate along a central ray, and propagation equations follow from our previous theory for $\boldsymbol{p}^{(R)} = \nabla\phi^{(R)}, \boldsymbol{p}^{(T)} = \nabla\phi^{(T)}$, $\boldsymbol{M}^{(R)} = \nabla\nabla\phi^{(R)}, \boldsymbol{M}^{(T)} = \nabla\nabla\phi^{(T)}$, where derivatives are evaluated along the central ray of the appropriate GWP, which must travel into the appropriate region, Ω^- or Ω^+.

Putting (6.3), (6.4) and (6.5) into (6.2a) we get

$$V^{(I)}\, \mathrm{e}^{\mathrm{i}\omega\phi^{(I)}} + V^{(R)}\, \mathrm{e}^{\mathrm{i}\omega\phi^{(R)}} = V^{(T)}\, \mathrm{e}^{\mathrm{i}\omega\phi^{(T)}} \quad \text{for } \boldsymbol{x} \text{ on } \bar{Z}(\cdot\,,\cdot). \tag{6.6}$$

Thus, to retain equality in (6.6) as $\omega \to \infty$, we take

$$\phi^{(I)}(\bar{Z}, t) = \phi^{(R)}(\bar{Z}, t) = \phi^{(T)}(\bar{Z}, t). \tag{6.7}$$

Now once $\phi^{(I)}$ is known, (6.7) and the eikonal equation (2.7) determine $\phi^{(R)}, \phi^{(T)}$ in Ω^-, Ω^+ respectively. That is, $\phi^{(R)}$ satisfies a first-order partial differential equation in four-dimensional space-time, with side conditions on the three-dimensional hypersurface $(\bar{Z}(\xi_1, \xi_2), t)$. This is analogous to giving initial conditions in three-dimensional space, and solving the eikonal equation to determine $\phi^{(R)}$ in space, for all time.

With $\phi^{(I)}$ given, we can in principle solve for, say, $\phi^{(R)}$ in Ω^- without the further paraxial approximation. We consider $\bar{Z}$ to have a global extension to C^3 as an analytic function of ξ_1, ξ_2. If $\phi^{(I)}$ is also an analytic function of complex $\boldsymbol{x}$, then (2.7) and (6.7) can be solved by complex ray tracing. At any point of complex $\bar{Z}$, and at any time t, a ray leaves the interface heading into Ω^-. Its initial direction, $\nabla\phi^{(R)}$, is determined by differentiating (6.7), that is,

$$\nabla\phi^{(R)}_{(\bar{Z},t)} \cdot \frac{\partial\bar{Z}}{\partial\xi_j} = \nabla\phi^{(I)}_{(\bar{Z},t)} \cdot \frac{\partial\bar{Z}}{\partial\xi_j}, \quad j = 1, 2. \tag{6.8}$$

Equation (6.8) determines two linearly independent components of $\nabla\phi^{(R)}$. The third component is obtained by differentiation of (6.7) with respect to t, and from (2.7)

$$c|\nabla\phi^{(R)}_{(\bar{Z},t)}| = -\phi^{(I)}_t(\bar{Z}, t). \tag{6.9}$$

Note that in (6.8) and (6.9), $\nabla\phi^{(I)}, \phi^{(I)}_t$ can be determined also by the complex ray theory for $\phi^{(I)}$; they are given by the corresponding quantities for the incident ray on $\bar{Z}$ at time t.

Now from (2.12), $\phi^{(I)}$ is conserved along the incident ray. From (6.7) this same value is picked up for $\phi^{(R)}$ i.e. the phase ϕ is conserved on reflection and transmission. By (2.12), ϕ is again conserved along reflected and transmitted rays. Thus, the field will be exponentially larger than anywhere else, when we follow the reflected and transmitted rays that are continuations of the incident ray for which $\operatorname{Im}\phi^{(I)} = 0$. That is, the reflected and transmitted GWPs have central rays that are excited when the central ray of the incident GWP strikes the interface. This happens, of course, in real space, and in general it is only these central rays that remain in real space for all time.

We next compute the paraxial approximation. We evaluate (6.8) and (6.9) at $\xi_1 = \xi_2 = 0$, at time t^* when the central ray of the incident GWP strikes the interface. From (6.1) we obtain

$$\left.\begin{aligned} \boldsymbol{p}^{(R)}\cdot\boldsymbol{t}_1 &= \boldsymbol{p}^{(I)}\cdot\boldsymbol{t}_1,\\ \boldsymbol{p}^{(R)}\cdot\boldsymbol{t}_2 &= \boldsymbol{p}^{(I)}\cdot\boldsymbol{t}_2,\end{aligned}\right\}\ \text{at } t = t^* \qquad c|\boldsymbol{p}^{(R)}| = 1. \tag{6.10}$$

Equation (6.10) is also obtained in ordinary ray theory. By standard arguments it implies the usual law of reflection. Similarly, Snell's law is derived from the equivalent conditions on the transmitted central ray

$$\left.\begin{aligned} \boldsymbol{p}^{(T)}\cdot\boldsymbol{t}_1 &= \boldsymbol{p}^{(I)}\cdot\boldsymbol{t}_1,\\ \boldsymbol{p}^{(T)}\cdot\boldsymbol{t}_2 &= \boldsymbol{p}^{(I)}\cdot\boldsymbol{t}_2,\end{aligned}\right\}\ \text{at } t = t^* \qquad c|\boldsymbol{p}^{(T)}| = 1. \tag{6.11}$$

Jump conditions for $\boldsymbol{M}^{(R)}$, $\boldsymbol{M}^{(T)}$ at t^*, in terms of $\boldsymbol{M}^{(I)}$, can now be constructed as conservation laws for the various components of $\boldsymbol{M} = \nabla\nabla\phi$. They arise naturally from second derivatives of (6.7), evaluated at $\xi_1 = \xi_2 = 0$. Hence, by using (2.15), we obtain that

$$c^2\bar{\boldsymbol{p}}^T\boldsymbol{M}\bar{\boldsymbol{p}} + \bar{\boldsymbol{p}}\cdot\nabla c \tag{6.12}$$

is conserved on reflection and transmission.

We differentiate (6.7) with respect to t, then with respect to $\xi_j, j = 1, 2$, to get two more conservation laws. After use of (2.7), and (6.1), evaluated at $\xi_1 = \xi_2 = 0$, we get

$$(\nabla c/c)\cdot\boldsymbol{t}_j + c\boldsymbol{t}_j^T\boldsymbol{M}\bar{\boldsymbol{p}}, \quad j = 1, 2, \tag{6.13}$$

is conserved on reflection and transmission.

Finally, three more conservation laws are derived by differentiation of (6.7) with respect to $\xi_j, \xi_l, j, l = 1, 2$:

$$\boldsymbol{t}_j^T\boldsymbol{M}\boldsymbol{t}_l + (2/c)\,(\bar{\boldsymbol{p}}\cdot\boldsymbol{t}_3)\,D_{jl}, \quad j, l = 1, 2, \tag{6.14}$$

is conserved on reflection and transmission.

Now (6.12), (6.13), (6.14) and the representation

$$\bar{\boldsymbol{p}} = \sum_{j=1}^{3} (\bar{\boldsymbol{p}}\cdot\boldsymbol{t}_j)\,\boldsymbol{t}_j \tag{6.15}$$

give six equations for the six components $\boldsymbol{t}_j^T\boldsymbol{M}\boldsymbol{t}_l, j, l = 1, 2, 3$. $\boldsymbol{M}$ can then be written by a change of basis.

It remains to derive jump conditions for the amplitudes, $V^{(R)}(\bar{Z}_0, t^*)$, $V^{(T)}(\bar{Z}_0, t^*)$. From (6.6) and (6.7) we obtain

$$V^{(I)} + V^{(R)} = V^{(T)}, \quad Z = \bar{Z}_0, \quad t = t^*. \tag{6.16}$$

From (2.1), (6.4), and (6.5), we obtain, to leading order in ω

$$\mu_-[V^{(I)}(\boldsymbol{p}^{(I)}\cdot\boldsymbol{t}_3) + V^{(R)}(\boldsymbol{p}^{(R)}\cdot\boldsymbol{t}_3)] = \mu_+[V^{(T)}(\boldsymbol{p}^{(T)}\cdot\boldsymbol{t}_3)]. \tag{6.17}$$

Now equations (6.16) and (6.17) arise also in ordinary ray theory. From the result that $c|\boldsymbol{p}| = 1$ for the central incident, reflected, and transmitted rays, and using Snell's law and the law of reflection, we obtain from (6.16) and (6.17) the usual reflection and transmission coefficients.

6.2. *Simplifications and general results*

We now analyse the jump conditions on the six elements of $\boldsymbol{M}$ given in (6.12)–(6.14). We use the ray vectors $\boldsymbol{e}_j, j = 1, 2, 3$ defined in §4, equation (4.3). We also refer $\boldsymbol{M}$ to this basis, via (4.6). Thus, we consider the six elements of the symmetric complex matrix $\bar{\boldsymbol{M}}$. We will show that a certain amount of decoupling occurs, i.e. the six jump conditions reduce to three sets of one, two and three equations, respectively.

We first define the matrix $\boldsymbol{S}$ as

$$S_{ij} = (1/c)\, \boldsymbol{t}_i \cdot \boldsymbol{e}_j, \quad i, j = 1, 2, 3. \tag{6.18}$$

Thus $c\boldsymbol{S}$ is unitary. We also define the vector $\boldsymbol{g}$ by

$$g_k = \boldsymbol{e}_k \cdot \nabla c, \quad k = 1, 2, 3. \tag{6.19}$$

The first decoupled equation is just (6.12), which we rewrite as

$$c^2 \bar{M}_{33} + g_3, \tag{6.20}$$

conserved on transmission and reflection. This isolates the (33) elements of $\bar{\boldsymbol{M}}$. The next set of coupled equations for $\bar{M}_{13}$ and $\bar{M}_{23}$ follow from (6.13) and (6.18)–(6.20). We get that

$$\sum_{k=1,\,2} S_{jk}[c^2 \bar{M}_{k3} + g_k], \quad j = 1, 2, \tag{6.21}$$

are conserved on transmission and reflection. Finally, we get a system of three coupled equations for $\bar{M}_{11}$, $\bar{M}_{12}$ and $\bar{M}_{22}$. These follow from (6.14), by using (6.18)–(6.21), as

$$\sum_{k,\,m=1,\,2} c^2 S_{jk} S_{lm} \bar{M}_{km} + 2S_{33} D_{jl} - [S_{j3} S_{l3} g_3 + \sum_{k=1,\,2} (S_{j3} S_{lk} + S_{l3} S_{jk})\, g_k], \qquad j, l = 1, 2, \tag{6.22}$$

conserved on transmission and reflections. Equations (6.22) are just the usual jump conditions for the wavefront curvatures of ordinary ray theory (Hubral 1980). Equations (6.21) and (6.20) are new; they consider quantities that are relevant only for GWPs, that do not enter into ordinary ray theory or the gaussian beam method (Popov 1982).

Consider, for example, incidence of a GWP at an interface between two homogeneous media. In addition, assume the incident GWP has one of its principal directions in the direction of propagation. Then, $\overline{M}_{k3} = 0, k = 1, 2$, for the incident GWP. Equation (6.21) then implies that $\overline{M}_{13} = \overline{M}_{23} = 0$ for both the reflected and transmitted GWPs. The reflected and transmitted GWPs thus still have principal axes along their respective propagation directions. This 'conservation of orientation' contrasts with the results of §5 for the simplest inhomogeneous medium with constantly varying acoustic properties. In that case, we saw that the principal axis and the ray direction, both initially aligned, tend to deviate from one another as the GWP propagates.

Finally, we note the jump conditions across an interface between homogeneous media in two dimensions, with wave speeds c_1 and c_2. Let the GWP be incident from medium 1, and make angle $\theta_1, 0 \leqslant \theta_1 < \frac{1}{2}\pi$, with the interface normal. The transmitted GWP makes an angle θ_2 with the normal, where $\sin\theta_2 = (c_2/c_1)\sin\theta_1$. The incident GWP is characterized by elements $\overline{M}_{11}^{(I)}$, $\overline{M}_{13}^{(I)}$ and $\overline{M}_{33}^{(I)}$. The reflected and transmitted GWP matrix elements are

$$\overline{M}_{33} = (c_1^2/c^2)\,\overline{M}_{33}^{(I)}, \tag{6.23a}$$

$$\overline{M}_{13} = \frac{c_1\cos\theta_1}{c\cos\theta}\,\overline{M}_{13}^{(I)}, \tag{6.23b}$$

$$\overline{M}_{11} = \frac{\cos^2\theta_1}{\cos^2\theta}\,\overline{M}_{11}^{(I)} + \frac{1}{\rho\cos^2\theta}\left(\frac{\cos\theta_1}{c_1} \mp \frac{\cos\theta}{c}\right). \tag{6.23c}$$

Here, the reflected (transmitted) matrix elements are given by taking $\theta = \theta_1(\theta_2), c = c_1(c_2)$ and the plus (minus) sign in (6.23c). The radius of curvature, ρ, of the interface, is positive (negative) if the centre of curvature lies in medium 2(1). Finally, in regard to (6.23a), we note the comment following (4.14).

6.3. *Numerical example*

We now illustrate the above analysis by applying the results to a simple problem of a GWP incident upon an obstacle. We consider a two-dimensional GWP in a homogeneous medium with wave speed c_1 that contains a circular region with a different wave speed c_2. The geometry of the scattering problem is shown in figure 6. The GWP is initially centred at A, at a distance r_0 from the centre of the circle of radius a. The initial pulse direction makes an angle θ with the line AB. The spatial distribution of the initial GWP about A is specified by $\overline{M} = \mathrm{diag}\,(\overline{m}_{10}, \overline{m}_{30})$.

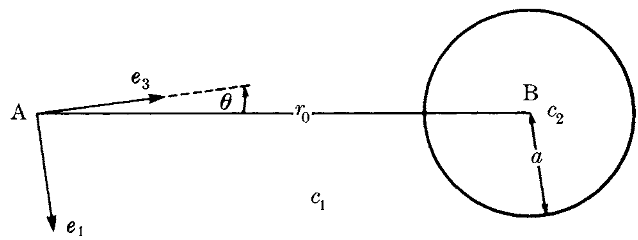

FIGURE 6. Geometry of the two-dimensional scattering problem.

value is picked up for $\phi^{(R)}$ i.e. the phase ϕ is conserved on reflection and transmission. By (2.12), ϕ is again conserved along reflected and transmitted rays. Thus, the field will be exponentially larger than anywhere else, when we follow the reflected and transmitted rays that are continuations of the incident ray for which $\operatorname{Im}\phi^{(I)} = 0$. That is, the reflected and transmitted GWPs have central rays that are excited when the central ray of the incident GWP strikes the interface. This happens, of course, in real space, and in general it is only these central rays that remain in real space for all time.

We next compute the paraxial approximation. We evaluate (6.8) and (6.9) at $\xi_1 = \xi_2 = 0$, at time t^* when the central ray of the incident GWP strikes the interface. From (6.1) we obtain

$$\left.\begin{aligned} \boldsymbol{p}^{(R)}\cdot\boldsymbol{t}_1 &= \boldsymbol{p}^{(I)}\cdot\boldsymbol{t}_1, \\ \boldsymbol{p}^{(R)}\cdot\boldsymbol{t}_2 &= \boldsymbol{p}^{(I)}\cdot\boldsymbol{t}_2, \end{aligned}\right\} \quad \text{at } t = t^* \qquad (6.10)$$

$$c|\boldsymbol{p}^{(R)}| = 1.$$

Equation (6.10) is also obtained in ordinary ray theory. By standard arguments it implies the usual law of reflection. Similarly, Snell's law is derived from the equivalent conditions on the transmitted central ray

$$\left.\begin{aligned} \boldsymbol{p}^{(T)}\cdot\boldsymbol{t}_1 &= \boldsymbol{p}^{(I)}\cdot\boldsymbol{t}_1, \\ \boldsymbol{p}^{(T)}\cdot\boldsymbol{t}_2 &= \boldsymbol{p}^{(I)}\cdot\boldsymbol{t}_2, \end{aligned}\right\} \quad \text{at } t = t^* \qquad (6.11)$$

$$c|\boldsymbol{p}^{(T)}| = 1.$$

Jump conditions for $\boldsymbol{M}^{(R)}$, $\boldsymbol{M}^{(T)}$ at t^*, in terms of $\boldsymbol{M}^{(I)}$, can now be constructed as conservation laws for the various components of $\boldsymbol{M} = \nabla\nabla\phi$. They arise naturally from second derivatives of (6.7), evaluated at $\xi_1 = \xi_2 = 0$. Hence, by using (2.15), we obtain that

$$c^2\overline{\boldsymbol{p}}^T\boldsymbol{M}\overline{\boldsymbol{p}} + \overline{\boldsymbol{p}}\cdot\nabla c \qquad (6.12)$$

is conserved on reflection and transmission.

We differentiate (6.7) with respect to t, then with respect to $\xi_j, j = 1, 2$, to get two more conservation laws. After use of (2.7), and (6.1), evaluated at $\xi_1 = \xi_2 = 0$, we get

$$(\nabla c/c)\cdot\boldsymbol{t}_j + c\boldsymbol{t}_j^T\boldsymbol{M}\overline{\boldsymbol{p}}, \quad j = 1, 2, \qquad (6.13)$$

is conserved on reflection and transmission.

Finally, three more conservation laws are derived by differentiation of (6.7) with respect to $\xi_j, \xi_l, j, l = 1, 2$:

$$\boldsymbol{t}_j^T\boldsymbol{M}\boldsymbol{t}_l + (2/c)(\overline{\boldsymbol{p}}\cdot\boldsymbol{t}_3)D_{jl}, \quad j, l = 1, 2, \qquad (6.14)$$

is conserved on reflection and transmission.

Now (6.12), (6.13), (6.14) and the representation

$$\overline{\boldsymbol{p}} = \sum_{j=1}^{3} (\overline{\boldsymbol{p}}\cdot\boldsymbol{t}_j)\,\boldsymbol{t}_j \qquad (6.15)$$

give six equations for the six components $\boldsymbol{t}_j^T\boldsymbol{M}\boldsymbol{t}_l, j, l = 1, 2, 3$. $\boldsymbol{M}$ can then be written by a change of basis.

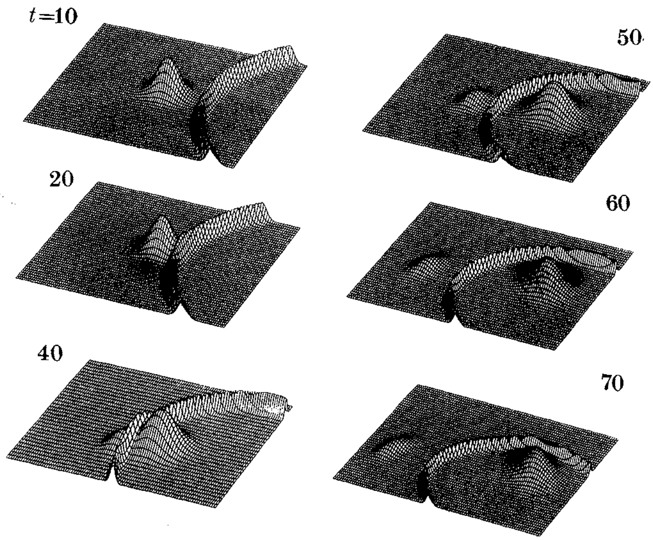

FIGURE 8. Scattering of a GWP from a cylindrical region of greater wave speed. The incident GWP strikes the interface at about $t = 30$. At later times, separate reflected and transmitted GWPs propagate.

7. CONCLUSION

The GWP may be thought of as a particle whose centre follows the ray trajectory of geometrical optics. At any instant in time, the particle is in the form of a specifically oriented ellipsoidally shaped disturbance. As it propagates, the particle never degenerates into a point; its finite size persists even at the geometrical caustics and foci of the rays. The particle size varies in such a way that it always maintains its initial total energy. These are the fundamental properties of a GWP in a smoothly varying medium.

All of the necessary parameters follow from a system of ordinary differential equations along the rays. The fundamental evolution equation is the classical ray equation, which could be derived from Fermet's principle. Equations for the GWP parameters then follow from the variational equations. We have derived the equations for the second-order spatial derivatives of the phase about the ray position. The second-order temporal derivative is given by (2.15), and the second-order mixed derivatives may be obtained easily. These quantities allow one to approximate the phase correct to second order, in both space and time about the ray $(\boldsymbol{y}(t), t)$. Higher-order variational equations would permit higher-order Taylor-series approximations. The evolution equations can be solved explicitly for a medium with a spatially constant velocity gradient. A GWP in such a medium rotates relative to the ray direction even as the ray itself rotates. This phenomenon may be interpreted through the concept of the packet as a bundle of rays, rather than as a particle. However, it is more than a bundle of neighbouring rays, because the GWP also accounts for the local behaviour of the disturbance in the ray direction.

The theory has also been extended to consider piecewise smooth media. The GWPs follow the standard laws of reflection and transmission at the surfaces of discontinuity. The theory as outlined would be adequate to treat, for example, the propagation of an acoustic pulse in a multilayered material. The theory could be adapted without much difficulty to consider ultrasonic-pulse propagation through elastic materials containing interfaces. However, a fully elastic theory should also include the effects of anisotropy. We defer until later a thorough discussion of the elastic problem.

Appendix A. Gaussian wave packets and the action principle

Consider the equation of motion for the field $u(\boldsymbol{x}, t)$

$$\theta u(\boldsymbol{x}, t) = 0, \tag{A 1}$$

where θ is the wave operator

$$\theta_{\mathrm{W}} = \rho\frac{\partial^2}{\partial t^2} - \nabla\rho c^2\nabla \tag{A 2}$$

or the Schrödinger operator

$$\theta_{\mathrm{S}} = \mathrm{i}\hbar\frac{\partial}{\partial t} + \frac{\hbar^2\nabla^2}{2m} - V(\boldsymbol{x}). \tag{A 3}$$

Above we have shown that in the high-frequency (high-energy) limit, a gaussian wave packet is an exact solution to (A 1) for suitable initial conditions. Asymptotics determine the equations of motion (2.9) for the centre $\boldsymbol{y}(t)$ and the momentum $\boldsymbol{p}(t)$ of the packet, and (2.27 a) governs the evolution of the complex width $\boldsymbol{M}(t)$.

Here we propose a general method to determine the parameters for all frequency. We note that the equation of motion (A 1) can be derived from the action (Hamilton's) principle

$$\frac{\delta S}{\delta u^*(\boldsymbol{x}, t)} = 0, \tag{A 4}$$

where θ is taken to be self adjoint and the action is

$$S = \int u^*(\boldsymbol{x}', t')\,\theta u(\boldsymbol{x}', t')\,\mathrm{d}\boldsymbol{x}'\,\mathrm{d}t'. \tag{A 5}$$

If u is a vector field, contraction over the spacial scripts is implied. Treating u^* and u as linearly independent, one immediately retrieves (A 1).

If $u(\boldsymbol{x}, t)$ is chosen to have a restricted form, for example a single GWP as in (2.29) or a linear combination of such packets, the parameters $\{\lambda_i(t)\}$ defining these functions are optimally fixed by minimizing the action S with respect to the parameters,

$$\frac{\delta S}{\delta \lambda_i^*(t)} = \frac{\delta \int u^*}{\delta \lambda_i^*(t)}(\boldsymbol{x}', t')\,\theta u(x', t')\,\mathrm{d}\boldsymbol{x}'\,\mathrm{d}t' = 0. \tag{A 6}$$

Treating λ_i and λ_i^* as independent variables, we obtain the equations of motion

$$\int \frac{\partial u^*(\boldsymbol{x}, t)}{\partial \lambda_i^*(t)}\,\theta u(\boldsymbol{x}, t)\,\mathrm{d}\boldsymbol{x} = 0. \tag{A 7}$$

For the wave equation, one obtains nonlinear equations involving second-time derivatives of the λs, whereas only first-time derivatives enter for the Schrödinger operator.

It is straightforward to show that in the high-frequency limit, the equations of motion for the GWP parameters $\boldsymbol{y}(t)$, $\boldsymbol{p}(t)$, $\boldsymbol{M}(t)$ and $V(t)$ are those given in §2. For general ω, the equations contain extra terms which in principle improve the GWP description of $u(\boldsymbol{x},t)$, for example by sampling the velocity $c(\boldsymbol{x})$ not only in the immediate vicinity of the ray $\boldsymbol{y}(t)$, but over a region of order the width of the gaussian about the ray. Important differences appear when $c(\boldsymbol{x})$ varies rapidly over the width, although the quality of the GWP solution depends on details of the problem being studied.

By way of illustration, we note that GWPs have been quite useful in quantum chemistry. As E. Heller (1975) and Drolshagen & Heller (1984) have stressed, in molecular photodissociation processes, GWPs not only lead to simplified calculations but also provide physical insight. Consider a diatomic molecule AB in its ground state. The wave function for the relative position $\boldsymbol{x}$ of A and B is initially $u_0(\boldsymbol{x})$, corresponding to the reduced mass moving in the effective potential $V_0(\boldsymbol{x})$. Suppose a photon of energy $\hbar\omega$ is absorbed by the molecule, exciting an electron by an energy $\hbar\omega_{\mathrm{ex}}$. The effective potential $V(\boldsymbol{x})$ in the excited state, being different from $V_0(\boldsymbol{x})$, causes $u(\boldsymbol{x},t)$ to vary with time. In particular, let us assume that $u_0(\boldsymbol{x})$ is well approximated by a gaussian of width a_0 centred at $\boldsymbol{y}_0$. Then if $V(\boldsymbol{x})$ is strongly repulsive, i.e. $\mathrm{d}V/\mathrm{d}x > 0$, the centre $\boldsymbol{y}(t)$ increases sufficiently rapidly that $a(t)$ remains essentially constant during the time t_1 it takes for the overlap

$$\hat{A}(t) = \int u_0^*(\boldsymbol{x},t)\,u(\boldsymbol{x},t)\,\mathrm{d}\boldsymbol{x} \tag{A 8}$$

to become small, $A(t_1) \ll 1$. The photodissociation cross section is proportional to the square of the Fourier transform of A,

$$\sigma(\omega)\propto|A(\omega-\omega_{\mathrm{ex}})|^2, \tag{A 9}$$

where
$$A(\omega-\omega_{\mathrm{ex}}) = \int_0^\infty A(t)\cos(\omega-\omega_{\mathrm{ex}})\,t\,\mathrm{d}t. \tag{A 10}$$

Therefore, $\sigma(\omega)$ reflects the power spectrum of the autocorrelation of the wave-function. Because $u(\boldsymbol{x},t)$ has a simple form for times of importance, a real-time description in terms of a GWP gives a clear picture of the process and explains the frequency dependence of $\sigma(\omega)$ in a transparent fashion. The more standard energy eigenfunction description of the photodissociation problem is considerably more complicated mathematically and less clear physically. In summary, the simplicity of a GWP description of the photodissociation process depends on (1) the initial state $u_0(\boldsymbol{x})$ being approximately gaussian and (2) the distortion of the packet being slow compared to the time for $u(\boldsymbol{x},t)$ to become spacially separated from $u_0(\boldsymbol{x})$.

In certain problems, like photoexcitation, the final state $u(\boldsymbol{x},t)$ is approximately a GWP that bounces back and forth in the potential well $V(\boldsymbol{x})$. In this case, $A(t)$ exhibits multiply periodic behaviour so that $\sigma(\omega)$ exhibits peaks at these frequencies, corresponding to excitation of $0, 1, 2, \ldots$ vibrational quanta in the final state.

More generally, $u(\boldsymbol{x}, t)$ may break into several packets, corresponding to reflected and transmitted waves at a classical turning point or in a region where $V(\boldsymbol{x})$ changes rapidly. In this case, several GWPs can be introduced with expansion coefficients $C_i(t)$ which change to take account of this bifurcation. This scheme has been used by Heller with fixed widths $a_i(t) = a_i(0)$ for each gaussian i. We note that the action principle permits one to optimally determine the coefficients $C_i(t)$ as well as the gaussian parameters.

In the past, a number of schemes have been proposed to determine the evolution of the parameters $\lambda_i(t)$. Heller exploited the fact that a gaussian remains gaussian when propagating in a harmonic potential. By retaining up to second-order terms in $\boldsymbol{x}-\boldsymbol{y}(t)$ in an expansion of $V(\boldsymbol{x}, t)$ about $\boldsymbol{y}(t)$ at each t, he found that the $\lambda_i(t)$ satisfy equations of motion analogous to those of the high frequency asymptotics, (2.9) and (2.27*a*). On the other hand, Sawada *et al.* (1985) proposed minimizing the error $x(\boldsymbol{x}, t)$ of the GWP solution

$$\chi(\boldsymbol{x}, t) \equiv \theta u_{\mathrm{G}}(\boldsymbol{x}, t). \tag{A 11}$$

This leads to

$$\frac{\delta}{\delta\lambda_i^*(t)}\int |\chi(\boldsymbol{x}, t)|^2\,\mathrm{d}\boldsymbol{x} = 0, \tag{A 12}$$

or

$$\int \frac{\partial u_{\mathrm{G}}^*(\boldsymbol{x}, t)}{\partial\lambda_i^*(t)}\theta^2 u(\boldsymbol{x}, t)\,\mathrm{d}\boldsymbol{x} = 0. \tag{A 13}$$

This is a result different than that (A 7) given by the action principle proposed above. Because θ^2 rather than θ appears, (A 13) is more complicated than (A 7) and we believe less accurate as well. We are currently studying several model problems to gain a better understanding of the advantages and limitations of the action-principle approach.

Appendix B. A wronskian result and some general results

We first derive a wronskian relation for later use. Let $(\boldsymbol{A}_1, \boldsymbol{B}_1)$ and $(\boldsymbol{A}_2, \boldsymbol{B}_2)$ be two distinct solutions to the system of equations (2.9) and (2.25) for the same initial data $\boldsymbol{y}_0, \boldsymbol{p}_0$ at $t = t_0$, but different initial values of $\boldsymbol{A}(t_0)$ and $\boldsymbol{B}(t_0)$. Then it may be shown quite easily from (2.25) that the wronskian

$$\boldsymbol{W}(t) = \boldsymbol{A}_1^T(t)\,\boldsymbol{B}_2(t) - \boldsymbol{B}_1^T(t)\,\boldsymbol{A}_2(t) \tag{B 1}$$

is constant, i.e. $\boldsymbol{W}(t) = \boldsymbol{W}(t_0)$. Because the coefficient matrices in (2.25) are all real, it follows that the real and imaginary parts of $\boldsymbol{A}(t)$ and $\boldsymbol{B}(t)$ propagate independently. Let

$$\boldsymbol{A}(t) = \boldsymbol{A}^{(1)}(t) + \mathrm{i}\boldsymbol{A}^{(2)}(t) \tag{B 2a}$$

$$\boldsymbol{B}(t) = \boldsymbol{B}^{(1)}(t) + \mathrm{i}\boldsymbol{B}^{(2)}(t), \tag{B 2b}$$

where $\boldsymbol{A}^{(1)}$, $\boldsymbol{A}^{(2)}$, $\boldsymbol{B}^{(1)}$, and $\boldsymbol{B}^{(2)}$ are real matrices. The wronskian result then implies a relation between these matrices.

The wronskian result with $(\boldsymbol{A}_1, \boldsymbol{B}_1) = (\boldsymbol{A}_2, \boldsymbol{B}_2) = (\boldsymbol{A}, \boldsymbol{B})$ implies that $\boldsymbol{A}^T(t)\,\boldsymbol{B}(t)$ is symmetric if and only if the initial matrix $\boldsymbol{A}^T(t_0)\,\boldsymbol{B}(t_0)$ is symmetric. Also, because

$$\boldsymbol{B}\boldsymbol{A}^{-1} = (\boldsymbol{A}^T)^{-1}\,(\boldsymbol{A}^T\boldsymbol{B})\,\boldsymbol{A}^{-1} \tag{B 3}$$

it follows that $\boldsymbol{M}(t) = \boldsymbol{B}\boldsymbol{A}^{-1}$ is symmetric if and only if $\boldsymbol{M}_0$ is symmetric.

Next, it is shown that the imaginary part of the matrix $\boldsymbol{M}$ is positive definite. This requires that $\boldsymbol{M}$ is symmetric, which is true, as shown above. Then,

$$\operatorname{Im}\boldsymbol{M} = \frac{1}{2\mathrm{i}}(\boldsymbol{B}\boldsymbol{A}^{-1} - (\boldsymbol{B}\boldsymbol{A}^{-1})^*), \tag{B 4}$$

where the asterisk denotes the adjoint (complex-conjugate transpose). Use of the wronskian result again gives

$$\begin{aligned}\boldsymbol{A}^*\operatorname{Im}(\boldsymbol{M})\,\boldsymbol{A} &= \frac{1}{2\mathrm{i}}(\boldsymbol{A}^*\boldsymbol{B} - \boldsymbol{B}^*\boldsymbol{A}) \\ &= \tfrac{1}{2}(\boldsymbol{L}_0 + \boldsymbol{L}_0^T),\end{aligned} \tag{B 5}$$

where

$$\boldsymbol{L}_0 = \boldsymbol{A}_0^{(1)T}\,\boldsymbol{B}_0^{(2)} - \boldsymbol{B}_0^{(1)T}\,\boldsymbol{A}_0^{(2)}. \tag{B 6}$$

Thus, $\boldsymbol{A}^*\operatorname{Im}(\boldsymbol{M})\,\boldsymbol{A}$ is real and constant. If we now impose the initial condition that $\boldsymbol{L}_0 + \boldsymbol{L}_0^T$ is positive definite, then it follows that $\boldsymbol{A}$ is non-singular. Therefore $\boldsymbol{A}^{-1}$ exists, and (2.20) shows that the amplitude V remains bounded everywhere in real space. In particular, there are no unphysical singularities at the geometrical caustics and foci of real rays. We also have from (B 5), that

$$\operatorname{Im}(\boldsymbol{M}) = (\boldsymbol{A}_0\boldsymbol{A}^{-1})^*\operatorname{Im}(\boldsymbol{M}_0)\,(\boldsymbol{A}_0\boldsymbol{A}^{-1}), \tag{B 7}$$

which implies that $\operatorname{Im}(\boldsymbol{M})$ is positive definite if $\operatorname{Im}(\boldsymbol{M}_0)$ is positive definite. This completes the proof. We note that it places no restrictions upon $\boldsymbol{A}_0$ and $\boldsymbol{B}_0$, except that $\boldsymbol{L}_0 + \boldsymbol{L}_0^T$ is positive definite. Alternatively, we can require that $\boldsymbol{A}_0^{-1}$ exists, and the only other requirements are that $\boldsymbol{M}_0$ is symmetric and that $\operatorname{Im}(\boldsymbol{M}_0)$ is positive definite, both of which are essential from physical arguments.

References

Berlanger, P. A. 1984 Packetlike solutions of the homogeneous wave equations. *J. opt. Soc. Am.* A **1**, 723–724.

Cerveny, V. 1983 Synthetic body wave seismograms for laterally varying structures by the Gaussian beam method. *Geophys. Jl R. astr. Soc.* **73**, 389–426.

Drolshagen, G. & Heller, E. J. 1984 Inelastic collisions without use of target states. *Chem. Phys. Lett.* **104**, 129–135.

Felsen, L. B. 1976 Evanescent waves. *J. opt. Soc. Am.* **66**, 751–760.

Hagedorn, G. A. 1984 A particle limit for the wave equation with variable wave speed. *Communs pure appl. Math.* **37**, 91–100.

Heller, E. J. 1975 Time dependent approach to semiclassical dynamics. *J. chem. Phys.* **62**, 1544–1555.

Hubral, P. 1980 Wavefront curvatures in three-dimensional laterally inhomogeneous media with curved interfaces. *Geophysics* **45**, 905–913.

Karal, F. C. & Keller, J. B. 1959 Elastic wave propagation in homogeneous and inhomogeneous media. *J. acoust. Soc. Am.* **31**, 694–703.

Keller, J. B. & Streifer, W. 1971 Complex rays with application to Gaussian beams. *J. opt. Soc. Am.* **61**, 40–43.

Michaels, P. 1977 Seismic raypath migration with the pocket calculator. *Geophysics* **42**, 1056–1063.

Norris, A. N. 1986 Complex point source representation of real point sources and the Gaussian beam summation method. *J. opt. Soc. Am.* A **3**, 2005–2010.

Popov, M. M. 1982 A new method of computation of wave fields using Gaussian beams. *Wave Motion* **4**, 85–97.

Popov, M. M. & Psencik, I. 1978 Computation of ray amplitudes in inhomogeneous media with curved interfaces. *Studia geophys. geod.* **16**, 248–258.

Sawada, S., Heather, R., Jackson, B. & Metiu, H. 1985 A strategy for time dependent quantum mechanical calculations using a Gaussian wave packet representation of the wave function. *J. chem. Phys.* **83**, 3009–3027.

Synge, J. L. 1972 A special class of solutions of the Schrödinger equation for a free particle. *Founds Phys.* **2**, 35–40.

Thomson, C. J. & Chapman, C. H. 1985 An introduction to Maslov's asymptotic method. *Geophys. Jl R. astr. Soc.* **83**, 143–168.

White, B. S., Burridge, R., Norris, A. N. & Bayliss, A. 1987 Some remarks on the Gaussian beam summation method. *Geophys. Jl R. astr. Soc.* (In the press.)